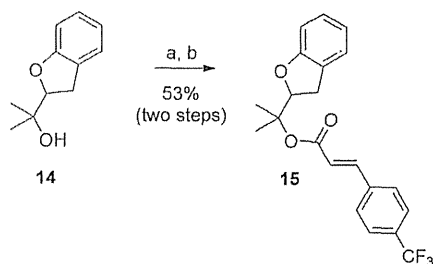Scheme 4. Synthesis of compound 13. *Reagents and conditions*: a) Triphosgene, DMAP, CH₂Cl₂, 1 h; b) benzylamine, ■ ■RT?■ ■, 16 h; then reflux, 16 h.

Scheme 5. Synthesis of compound 15. *Reagents and conditions*: a) Meldrum's acid, toluene, reflux, 7 h; b) 4-(trifluoromethyl)benzaldehyde, piperidine, pyridine, 70 °C, 12 h.

Table 1. Structure–activity relationship data against PANC-1 cells under nutrient-deprived conditions.[35]

Compound	$PC_{50}^{[a]}$ [nM]	Compound	$PC_{50}^{[a]}$ [nM]
(±)-angelmarin (6)	91 (8)	8m	730 (84)
(±)-columbianetin (4)	inactive[b,c]	8n	inactive[b]
8a	310 (72)	8o	7100 (720)
8b	10 (3)	8p	610 (97)
8c	5000 (560)	8q	140 (35)
8d	270 (15)	8r	79 (5)
8e	120 (34)	8s	310 (41)
8f	250 (22)	8t	320 (55)
8g	1000 (480)	9	inactive[b]
8h	2500 (740)	10	440 (76)
8i	23 (2)	11	inactive[b]
8j	inactive[b]	13	25000 (5400)
8k	inactive[b]	15	3600 (780)
8l	700 (120)		

[a] Preferential cytotoxicity (PC_{50}) corresponds to the IC_{50} value in nutrient-deprived medium for a compound that shows no cytotoxicity towards PANC-1 cells cultured in a nutrient-rich medium. Standard deviations are given in parentheses ($n=4$). [b] No observed toxicity in nutrient-deprived medium at the highest test concentration of 10 mg mL⁻¹. [c] Columbianetin was previously evaluated in this assay, see Ref. [25].

could potentially act as a prodrug with increased cell permeability, a hypothesis that is undergoing further investigation. Masking of the phenol moiety as the corresponding methyl ether, as in analogue 8c resulted in a considerable loss of cytotoxicity ($PC_{50}=5000$ nM), while replacing the phenolic hydroxy group with a methyl substituent (compounds 8d) resulted in a threefold activity decrease (c.f., compound 6). Two aminecontaining analogues were examined; dimethylamino ana-

logue 8e exhibits similar activity to the natural product ($PC_{50}=120$ nM), whereas acetamide 8f is inferior ($PC_{50}=250$ nM) and 20-fold less potent than the analogous acetate ester (8b). 4-Fluoro- and 4-chloro-substituted analogues 8g and 8h, respectively, were active only at micromolar concentrations, with PC_{50} values of 1000 and 2500 nM, respectively. Interestingly, 2-fluoro derivative 8p ($PC_{50}=610$ nM) and 3,5-difluoro derivative 8q ($PC_{50}=140$ nM) were both more cytotoxic than 4-fluoro analogue 8g, with 8q exhibiting similar potency to (±)-angelmarin (6).■ ■ok? or should this be (+)-angelmarin?■ ■

We were gratified to discover that replacement of the phenol hydroxy moiety of angelmarin (6) with a trifluoromethyl substituent (analogue 8i) resulted in a fourfold increase in potency ($PC_{50}=23$ nM). Curiously, other electron-withdrawing substituents in place of the trifluoromethyl, such as nitrile (8j) and nitro (8k) groups, resulted in a complete loss of cytotoxicity. Notably, *meta*-trifluoromethyl-substituted analogue 8r is also highly potent ($PC_{50}=79$ nM). Detailed rationalisation of these results is limited by the whole-cell nature of the assay and the lack of information on the mechanism of action and biological target(s), and further studies are required to gain additional insight■ ■ok?■ ■.

Transposition of the phenolic hydroxy group of angelmarin to the *meta* position (8l) resulted in an approximately eightfold decrease in preferential cytotoxicity. 3,4-Dihydroxy analogue 8m showed a similar decrease in activity. 2,3,4-Trimethoxyphenyl derivative 8n was inactive, while 3-cyano derivative 8o was weakly active, with a PC_{50} value of 7100 nM. Finally, replacing the phenyl ring with two heterocycles, furan 8s and pyridine 8t, resulted in decreased but still sub-micromolar cytotoxicity.

2′,3′-Dihydroangelmarin analogue 10 displayed a fivefold decrease in preferential cytotoxicity ($PC_{50}=440$ nM) in comparison with (±)-angelmarin (6), suggesting that either conformational rigidity associated with the *E* olefin or conjugation are important for highly potent antiausterity activity, but that this conjugated double bond is not absolutely essential. Further hydrogenation to the 3,4,2′,3′-tetrahydro derivative (11) eliminated activity completely, highlighting the significance of the intact coumarin ring system. By comparison, truncated 2,3-dihydrobenzofuran 15, which lacks the coumarin portion of angelmarin but includes the *para*-trifluoromethyl substituent (effectively incorporated into 8i) showed only modest antiausterity activity ($PC_{50}=3600$ nM). Interestingly, carbamate 13 displayed weak activity ($PC_{50}=25000$ nM), suggesting that investigation of alternatives to the ester linkage could give interesting results.

Figure 1 depicts antiausterity activity dose–response curves for the most active analogues, compounds 8b and 8i, compared with (±)-angelmarin (6). Importantly, as illustrated for 8b and 8i in Figure 1, all of the active compounds tested (see Table 1) inhibit PANC-1 cells in NDM but not in normal growth medium (i.e., DMEM), thus displaying the necessary preferential cytotoxicity for the antiausterity strategy. Notably, all of the compounds were tested as the racemate, and so more potent activities might be expected for the corresponding pure enantiomers.■ ■ok?■ ■

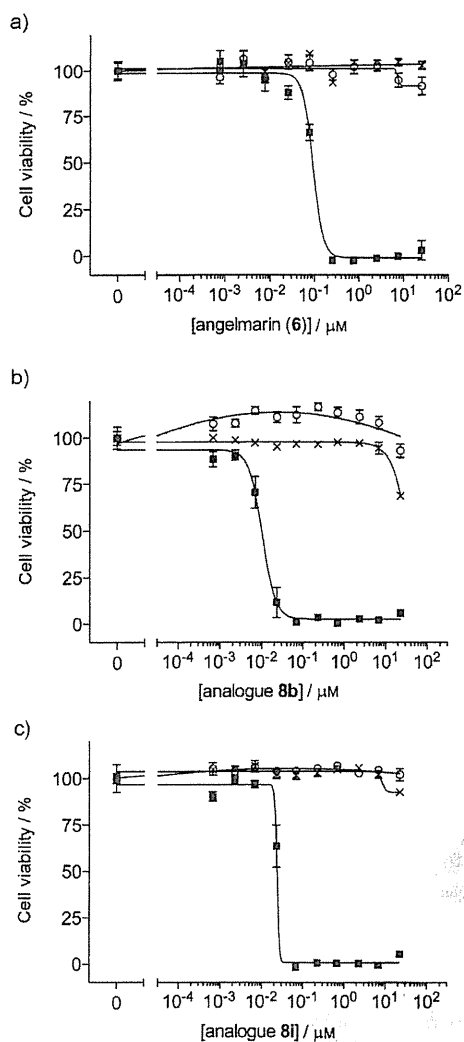These are not the final page numbers! ↗↗

a)

b)

c)

Figure 1. Cell viability versus concentration of a) (±)-angelmarin (6), b) acetate ester 8b and c) trifluoromethyl analogue 8i evaluated in PANC-1 cells grown in nutrient-deprived medium (NDM, ■) versus those cultured in normal growth medium (DMEM, ○ and ×). Cell viability was determined after incubation for 24 h. Measurements were performed in quadruplicate, and data shown are the mean ± standard error of the mean (SEM). ■ ■ Caption ok? ■ ■

In conclusion, a number of analogues of the potent antiausterity, anticancer natural product angelmarin have been synthesised and evaluated for their ability to inhibit the tolerance of PANC-1 cells to survive nutrient deprivation. We have elucidated preliminary structure–activity relationships, mainly focused on the *para*-hydroxycinnamate subunit of the natural product. Three analogues synthesised (8b, 8i and 8r) exhibit superior antiausterity activity compared with the racemic natural product 6. The most potent of the novel compounds was acetate ester 8b, which possibly acts as a prodrug with improved cell permeability. Compounds 8i and 8r feature trifluoromethyl substituents in the *para* and *meta* positions, with the *para*-substituted compound being the more potent. Preliminary results suggest the *E* cinnamate double bond is important for potent activity but not essential, whereas changes

to the coumarin moiety were not tolerated. The compounds described here provide a basis for the design of future analogues as molecular probes to undertake mechanism of action and target(s) identification studies. These efforts are underway and will be reported in due course.

Experimental Section

Antiausterity assay: Human pancreatic carcinoma, epithelial-like cells (PANC-1) ■ ■ ok? ■ ■ were seeded in 96-well plates (1×10^4 per well) and incubated in fresh Dulbecco's modified Eagle's medium (DMEM) at 37 °C in an atmosphere of 5% CO_2/95% air for 24 h. The cells were then washed with phosphate-buffered saline (PBS), and the medium was changed to either DMEM or nutrient-deprived medium (NDM; absence of glucose, amino acid, and serum), followed by immediate addition of serial dilutions of the test samples. After 24 h incubation, the cells were washed again with PBS, then DMEM (100 µL) with 10% WST-8 cell counting kit solution was added to the wells, and the plate was incubated for a further 2 h. Then, the absorbance of the wells at 450 nm was measured. The viable cell number was determined using a previously prepared calibration curve. None of the analogues evaluated were cytotoxic to PANC-1 cells cultured in DMEM medium up to 10 mg mL^{-1}. PC_{50} values correspond to the IC_{50} values in nutrient-deprived medium; these were calculated based on nonlinear regression analysis of dose–response data (fitting data to four-parameter sigmoidal model) using GraphPad Prism version 5.0d for Mac OS X.

General procedure for the preparation of 6 and 8a–t: A solution of (±)-columbianetin[34] (1.0 equiv) in toluene (10 mL mmol^{-1} substrate) was treated with 2,2-dimethyl-1,3-dioxane-4,6-dione (1.0 equiv) and heated at reflux for 7 h, at which point TLC analysis indicated complete consumption of starting material. The reaction mixture was cooled to RT and concentrated in vacuo to yield crude carboxylic acid 5 as a yellow oil, which was immediately redissolved in pyridine (10 mL mmol^{-1} substrate). Piperidine (1 drop m-mol^{-1} substrate) and appropriate benzaldehyde 7 (1.1 equiv) were added, and the reaction mixture was heated at 70 °C for 16 h. After cooling to RT, the reaction mixture was diluted with EtOAc and washed with 5% aq HCl, water, brine. The organic phase was dried over MgSO$_4$, filtered and concentrated in vacuo. The crude product was purified by flash column chromatography (gradient elution with EtOAc in petroleum spirits). Details of synthetic procedures and compound characterisation are provided in the Supporting Information.

[1] R. M. Sutherland, *Science* **1988**, *240*, 177–184.
[2] P. Vaupel, F. Kallinowski, P. Okunieff, *Cancer Res.* **1989**, *49*, 6449–6465.

[3] K. Koito, T. Namieno, T. Nagakawa, K. Morita, *AJR, Am. J. Roentgenol.* **1997**, *169*, 1263–1267.

[4] K. Ranniger, R. M. Saldino, *Radiology* **1966**, *86*, 470–474.

[5] N. A. Yassa, J. Yang, S. Stein, M. Johnson, P. Ralls, *J. Clin. Ultrasound* **1997**, *25*, 473–480.

[6] T. Y. Reynolds, S. Rockwell, P. M. Glazer, *Cancer Res.* **1996**, *56*, 5754–5757.

[7] J. Yuan, L. Narayanan, S. Rockwell, P. M. Glazer, *Cancer Res.* **2000**, *60*, 4372–4376.

[8] J. Yun, A. Tomida, K. Nagata, T. Tsuruo, *Oncol. Res.* **1995**, *7*, 583–590.

[9] A. Tomida, J. Yun, T. Tsuruo, *Int. J. Cancer* **1996**, *68*, 391–396.

[10] J. Folkman, *N. Engl. J. Med.* **1971**, *285*, 1182–1186.

[11] D. E. Richard, E. Berra, J. Pouyssegur, *Biochem. Biophys. Res. Commun.* **1999**, *266*, 718–722.

[12] P. E. Thorpe, *Clin. Cancer Res.* **2004**, *10*, 415–427.

[13] W. E. Fisher, D. H. Berger, *Int. J. Gastrointest. Cancer* **2003**, *33*, 79–88.

[14] J. B. Fleming, R. A. Brekken, *J. Cell. Biochem.* **2003**, *90*, 492–501.

[15] M. Korc, *Mol. Cancer* **2003**, *2*, 8.

[16] D. Wei, X. Le, L. Zheng, L. Wang, J. A. Frey, A. C. Gao, Z. Peng, S. Huang, H. Q. Xiong, J. L. Abbruzzese, K. Xie, *Oncogene* **2003**, *22*, 319–329.

[17] A. Masamune, K. Kikuta, T. Watanabe, K. Satoh, M. Hirota, T. Shimosegawa, *Am. J. Physiol. Gastrointest. Liver Physiol.* **2008**, *295*, G709–717.

[18] K. Izuishi, K. Kato, T. Ogura, T. Kinoshita, H. Esumi, *Cancer Res.* **2000**, *60*, 6201–6207.

[19] J. Magolan, M. J. Coster, *Curr. Drug Delivery* **2010**, *7*, 355–369.

[20] H. Esumi, J. Lu, Y. Kurashima, T. Hanaoka, *Cancer Sci.* **2004**, *95*, 685–690.

[21] J. Lu, S. Kunimoto, Y. Yamazaki, M. Kaminishi, H. Esumi, *Cancer Sci.* **2004**, *95*, 547–552.

[22] S. Awale, J. Lu, S. K. Kalauni, Y. Kurashima, Y. Tezuka, S. Kadota, H. Esumi, *Cancer Res.* **2006**, *66*, 1751–1757.

[23] P. Turner, E. Griffin, J. Whatmore, M. Shipman, *Org. Lett.* **2011**, *13*, 1056–1059.

[24] T. Devji, C. Reddy, C. Woo, S. Awale, S. Kadota, D. Carrico-Moniz, *Bioorg. Med. Chem. Lett.* **2011**, *21*, 5770–5773.

[25] S. Awale, E. M. Nakashima, S. K. Kalauni, Y. Tezuka, Y. Kurashima, J. Lu, H. Esumi, S. Kadota, *Bioorg. Med. Chem. Lett.* **2006**, *16*, 581–583.

[26] N. N. Win, S. Awale, H. Esumi, Y. Tezuka, S. Kadota, *J. Nat. Prod.* **2007**, *70*, 1582–1587.

[27] N. N. Win, S. Awale, H. Esumi, Y. Tezuka, S. Kadota, *Bioorg. Med. Chem. Lett.* **2008**, *18*, 4688–4691.

[28] N. N. Win, S. Awale, H. Esumi, Y. Tezuka, S. Kadota, *Bioorg. Med. Chem.* **2008**, *16*, 8653–8660.

[29] N. N. Win, S. Awale, H. Esumi, Y. Tezuka, S. Kadota, *Chem. Pharm. Bull.* **2008**, *56*, 491–496.

[30] S. Awale, F. Li, H. Onozuka, H. Esumi, Y. Tezuka, S. Kadota, *Bioorg. Med. Chem.* **2008**, *16*, 181–189.

[31] F. Li, S. Awale, Y. Tezuka, S. Kadota, *Bioorg. Med. Chem.* **2008**, *16*, 5434–5440.

[32] S. Awale, T. Miyamoto, T. Z. Linn, F. Li, N. N. Win, Y. Tezuka, H. Esumi, S. Kadota, *J. Nat. Prod.* **2009**, *72*, 1631–1636.

[33] F. Li, S. Awale, H. Zhang, Y. Tezuka, H. Esumi, S. Kadota, *J. Nat. Prod.* **2009**, *72*, 1283–1287.

[34] J. Magolan, M. J. Coster, *J. Org. Chem.* **2009**, *74*, 5083–5086.

[35] H. Jiang, Y. Hamada, *Org. Biomol. Chem.* **2009**, *7*, 4173–4176.

[36] E. B. J. Harris, M. G. Banwell, A. C. Willis, *Tetrahedron Lett.* **2011**, *52*, 6887–6889.

[37] D. J. Clarke, R. S. Robinson, *Tetrahedron* **2002**, *58*, 2831–2837.

[38] Compound **9** was inactive in the antiausterity assay. Six analogues (**8a,g,h,k,p,s**) could not be separated from **9** via column chromatography (see supporting information). In these cases, a mixture of the analogue and **9** (minor component, composition determined by ^{1}H NMR) was evaluated in the assay and the results were corrected accordingly.

[39] H. Zhao, C. Lee, P. Sai, Y. H. Choe, M. Boro, A. Pendri, S. Guan, R. B. Greenwald, *J. Org. Chem.* **2000**, *65*, 4601–4606.

[40] W. A. Henne, D. D. Doorneweerd, A. R. Hilgenbrink, S. A. Kularatne, P. S. Low, *Bioorg. Med. Chem. Lett.* **2006**, *16*, 5350–5355.

[41] S. B. Damle, *Chem. Eng. News* **1993**, *71*, 4–5.

[42] Compound **8b** was prepared via acetylation of (±)-angelmarin (**6**), as detailed in the Supporting Information.

COMMUNICATIONS

J. Magolan, N. B. P. Adams, H. Onozuka,
*N. L. Hungerford, H. Esumi, M. J. Coster**

■■ – ■■

🖥 **Synthesis and Evaluation of Anticancer Natural Product Analogues Based on Angelmarin: Targeting the Tolerance towards Nutrient Deprivation**

SAR ⟹

(±)-Angelmarin
$PC_{50} = 91$ nM

Analogue 8b
$PC_{50} = 10$ nM
Analogue 8i
$PC_{50} = 23$ nM
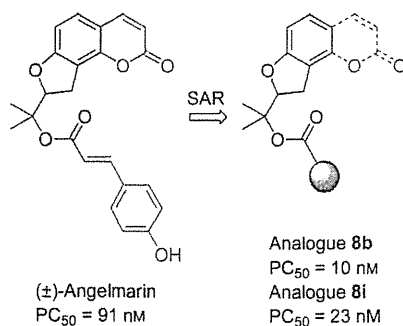
Inspired by nature: Angelmarin is an anticancer, natural product with potent antiausterity activity, that is, selective cytotoxic towards nutrient-deprived, resistant cancer cells. Through structure–activity relationship studies, three analogues were identified as lead compounds for the develpoment of molecular probes for the investigation of the mode of action and biological targets of the antiausterity strategy.■ ■Text ok? ■■

🖒🖒 **These are not the final page numbers!**

An anticancer agent, pyrvinium pamoate inhibits the NADH–fumarate reductase system—a unique mitochondrial energy metabolism in tumour microenvironments

Eriko Tomitsuka[1,2,*†], Kiyoshi Kita[2] and Hiroyasu Esumi[1,3]

[1]Cancer Physiology Project, Research Center for Innovative Oncology, National Cancer Center Hospital East, 6-5-1 Kashiwanoha, Kashiwa, Chiba 277-8577; [2]Department of Biomedical Chemistry, Graduate School of Medicine, The University of Tokyo, 7-3-1 Hongo, Bunkyo-ku, Tokyo 113-0033; and [3]National Cancer Center Research Institute, 5-1-1 Tsukiji, Chuo-ku, Tokyo 104-0045, Japan

*Eriko Tomitsuka, Cancer Physiology Project, Research Center for Innovative Oncology, National Cancer Center Hospital East, 6-5-1 Kashiwanoha, Kashiwa, Chiba 277-8577, Japan email: e-tomi@humeco.m.u-tokyo.ac.jp; Tel/Fax: +81-4-7134-8786

†Present address: Eriko Tomitsuka, Department of Human Ecology, Graduate School of Medicine, The University of Tokyo, 7-3-1 Hongo, Bunkyo-ku, Tokyo 113-0033, Japan

Increased glycolysis is the principal explanation for how cancer cells generate energy in the absence of oxygen. However, in actual human tumour microenvironments, hypoxia is often associated with hypoglycemia because of the poor blood supply. Therefore, glycolysis cannot be the sole mechanism for the maintenance of the energy status in cancers. To understand energy metabolism in cancer cells under hypoxia–hypoglycemic conditions mimicking the tumour microenvironments, we examined the NADH–fumarate reductase (NADH–FR) system, which functions in parasites under hypoxic condition, as a candidate mechanism. In human cancer cells (DLD-1, Panc-1 and HepG2) cultured under hypoxic–hypoglycemic conditions, NADH–FR activity, which is composed of the activities of complex I (NADH–ubiquinone reductase) and the reverse reaction of complex II (quinol–FR), increased, whereas NADH-oxidase activity decreased. Pyrvinium pamoate (PP), which is an anthelmintic and has an anti-cancer effect within tumour-mimicking microenvironments, inhibited NADH–FR activities in both parasites and mammalian mitochondria. Moreover, PP increased the activity of complex II (succinate–ubiquinone reductase) in mitochondria from human cancer cells cultured under normoxia–normoglycemic conditions but not under hypoxia–hypoglycemic conditions. These results indicate that the NADH–FR system may be important for maintaining mitochondrial energy production in tumour microenvironments and suggest its potential use as a novel therapeutic target.

Keywords: complex I/complex II/NADH–fumarate reductase system/pyrvinium pamoate/tumour microenvironments.

Abbreviations: ΔΨm, mitochondrial membrane potential; ETC, electron transport chain; NADH–FR, NADH–fumarate reductase; NADH–RQR, NADH–rhodoquinone reductase; NADH–UQR, NADH–ubiquinone reductase; PA, pamoic acid; PP, pyrvinium pamoate; QFR, quinol–fumarate reductase; SDH, succinate dehydrogenase; SQR, succinate–ubiquinone reductase; UQ, ubiquinone.

When adequate oxygen is supplied to tissue, ATP is mainly generated by oxidative phosphorylation through the electron transport chain (ETC) in the mitochondria of most human tissues. In normal tissues, the oxygen concentration is well maintained by physiological responses. In tumour tissues, on the other hand, the oxygen concentration is known to be heterogeneous both topologically and temporally and in general is relatively and sometimes extremely low (1, 2). Moreover, in hypovascular tumours, such as pancreatic cancer, the deprivation of both oxygen and nutrients occurs as a result of the limited blood supply to the tumour tissues. Reportedly, the glucose concentration is markedly lower in tumour tissues than in normal tissues (3). However, cancer cells are known to obtain energy mainly by glycolysis, as observed by the increase in glucose uptake and lactate production, known as the Warburg effect (4). As some cancer cells do not show a high activity of glycolysis (5) and the quantity of glucose is restricted in hypovascular tumours, Warburg effect alone cannot explain how cancer cells sustain their required energy levels under such conditions.

When tumour microenvironments are mimicked by the withdrawal of nutrients and oxygen, cancer cells become resistant to conventional chemotherapeutics. Lu et al. (6) have shown that traditional anticancer agents, such as 5-FU and cisplatin, exhibit cytotoxicity in normal medium but only minimal effects in nutrient-free medium. Under hypoxic condition, cancer cells have been shown to become resistant to some anticancer agents, such as bleomycin and vincristine (7). The molecular mechanism for hypoxia-induced drug resistance is not well understood, but the development of anticancer agents effective under nutrient-starved and hypoxic conditions or even specifically effective under such conditions is mandatory (8).

In this regard, we have reported on several anticancer agents that exert cytotoxic effects selectively
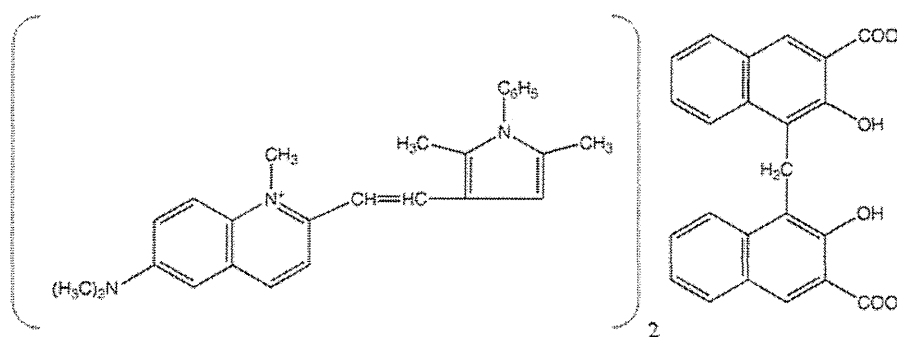
Fig. 1 Structural formula for pyrvinium pamoate.

under nutrient-depleted conditions mimicking tumour microenvironments. Kigamicin D and arctigenin are highly cytotoxic in nutrient-free medium and exhibit antitumour activities (*6, 9*). Pyrvinium pamoate (PP; Fig. 1), an anthelmintic also showed an anti-cancer activity against human cancer cells (*10*). Parasitic helminths live in the intestines of their mammalian hosts, where the oxygen concentration is relatively low and they use the phosphoenolpyruvate carboxykinase (PEPCK)-succinate pathway for hypoxic energy production. The final step in this pathway is the NADH—fumarate reductase (NADH—FR) system (*11*). PP is considered an effective and useful anthelmintic for pinworm infections when administered orally and a single dose of 5 mg per kg body weight in adult humans is highly effective (*12*). The inhibitory effect of PP on pinworms is thought to occur as a result of interference with glucose absorption in parasites (*13*). In addition, the mechanism responsible for the inhibitory effect of PP is thought to result from the inhibition of mitochondrial fumarate reductase (FRD) activity (*13*). Recently, PP has been shown to exhibit anti-parasitic activities against some parasite infections, such as cryptosporidiosis and malaria (*14, 15*), as well as an anticancer-effect on human cancer cell xenografts (*10, 16, 17*). However, the mechanisms of these effects have not been fully elucidated. In human cultured cells, PP also showed some pharmacological effects, including the inhibition of androgen receptors and the dependent gene transcription inhibition of ER stress, leading to cell death (*18*).

In this report, at first, to clarify the function of ETC in tumour microenvironments, activity changes in normoxic and hypoxic ETCs were compared. Next, to clarify the mechanisms of the anti-parasitic and anti-cancer effects of PP in parasites and mammals, respectively, the effects on enzyme activities in the ETC of helminths and mammals were examined. Thirdly, to understand how and why PP exhibits an anticancer activity specifically within tumour microenvironments, the effects of PP on mitochondrial energy metabolism under normal and tumour-microenvironment-mimicking conditions were compared. Finally, we investigated the mechanism of the action of PP on one of the mitochondrial ETC enzymes, complex II.

Materials and Methods

Materials

PP, pamoic acid (PA), ubiquinone-1 and ubiquinone-2 were purchased from Sigma. Sucrose monolaurate was purchased from Iwai Chemicals. Decyl-rhodoquinone was synthesized as described (*19*). All other chemicals were purchased from Wako and Sigma.

Cell culture

Human pancreatic cancer cells (Panc-1) and human hepatocellular carcinoma cells (HepG2) were cultured in DMEM (GIBCO BRL), human colorectal adenocarcinoma cells (DLD-1) were cultured in RPMI-1640 (GIBCO BRL) and human dermal fibroblast cells (HDF: TOYOBO) were cultured in DMEM/F12 (GIBCO BRL) supplemented with 10% heat-inactivated foetal bovine serum (Tissue Culture Biochemicals) and antibiotics in $75 \, cm^2$ tissue culture flasks (CORNING) under 5% CO_2 at 37°C. All the cells except for HDF were purchased from ATCC. All cells were maintained under normal conditions. After 3 days, the medium was changed for glucose depleted, glucose and glutamine-free DMEM (Sigma) with 10% heat-inactivated dialysed foetal bovine serum, and for hypoxia, the cells were cultured in an atmosphere of 5% CO_2, 1% O_2 and 94% N_2 at 37°C. To collect all cells, detaching cells were trypsinized and floating cells in cultured medium were centrifuged and all cells were counted with a Cell Countess™ automated cell counter according to the manufacturer's protocol (Invitrogen). Viable cells and dead cells were identified by dye-exclusion with trypan blue.

Preparation of mitochondria

Mitochondria were prepared from cultured cells as described previously (*20*). The mitochondrial proteins were solubilized with 2.5% (w/v) sucrose monolaurate. 1/100 volume of protease inhibitor cocktail (Sigma), 1 mM sodium malonate and 1/100 volume of phosphatase inhibitors I and II (Sigma) and were stirred on ice for 1 h. After centrifugation at 72,000 × *g* for 20 min at 4°C, the supernatant was subjected to 2D gel electrophoresis or phosphatase treatment.

Ascaris suum mitochondria were prepared from the muscle of adult *A. suum* as described previously (*21*). Bovine submitochondrial particles were prepared from bovine heart as described previously (*22*).

The protein concentrations were estimated using the Bradford method (*23*).

Enzyme assays

The mitochondrial activities of succinate dehydrogenase (SDH) (*24*), succinate ubiquinone reductase (SQR) (*25*), quinol—fumarate reductase (QFR), NADH—FR, NADH—ubiquinone reductase (NADH—UQR) and NADH—rhodoquinone reductase (NADH—RQR) (*25, 26*) were assayed as described previously. All the assays were performed at 25°C except for the NADH—FR assay (performed at 30°C) using 50 mM potassium phosphate (pH 7.5) as a reaction buffer. PP and PA were incubated with mitochondrial samples in a reaction buffer for 5 min at 25°C before the addition of the substrate.

Measurement of mitochondrial oxygen consumption

Mitochondrial oxygen consumption was measured using a Biological Oxygen Monitor 5300 (Yellow Spring Instrument) with

Clark type oxygen electrodes (27). Potassium phosphate (50 mM, pH 7.5) was used as a reaction buffer. Bovine submitochondrial particles (100 μg/mL) and PP were added and the reaction was started by the addition of 5 mM of potassium succinate or 1 mM of NADH as a substrate.

2D polyacrylamide gel electrophoresis

2D gel electrophoresis was performed as described previously (20). Solubilized mitochondrial proteins and 9.2 M urea, 1% (w/v) sucrose monolaurate, 0.6% (w/v) DTT, 2% (v/v) IPG buffer, a small amount of Orange G and a pI marker (BDH; Range 5.65~8.3) were added and run on an IPGphor isoelectric focusing unit (GE Healthcare) according to the manufacturer's protocol. For the second dimension, the strips were equilibrated with SDS–PAGE running buffer for 5 min at room temperature and then applied to 12.5% polyacrylamide gels and analysed using immunoblotting.

Treatment with phosphatase

For the phosphatase treatment, the solubilized mitochondrial proteins in Antarctic Phosphatase buffer containing protease inhibitor cocktails were treated with Antarctic Phosphatase (BioLabs) at 37°C for 2 h. For the phosphatase treatment negative control, 1/100 volumes of phosphatase inhibitors I and II were added (20).

Measurement of mitochondrial membrane potentials

Freshly prepared mitochondria were suspended at a concentration of 1 mg protein/mL in 220 mM sucrose, 68 mM mannitol, 10 mM potassium chloride, 5 mM KH_2O_4, 2 mM $MgCl_2$, 0.5 mM EGTA and 10 mM HEPES (pH 7.4). One hundred microlitres of the samples was poured on a 96-well plate and 5 μM of Rhodamine 123 was added. The fluorescence emission was monitored at room temperature using 538 nm as the emission wavelength and 485 nm as the excitation wavelength for 5 min (10 counts/min) in Asent Fluoroskan (Labsystem). Mitochondrial membrane potential ($\Delta\Psi m$) build-up was stimulated by the addition of 1 mM sodium succinate or 1 mM sodium fumarate as a substrate and incubated for 5 min, then measured for 5 min. Sodium cyanide (10 mM) was added as the inhibitor of complex IV, 0.5 μM PP was added after the addition of the substrates and the samples were incubated and measured for 5 min each. Finally, 100 nM of carbonyl cyanide-p-trifluoromethoxyphenylhydrazone (FCCP), a mitochondrial uncoupling reagent, was added to collapse the formed membrane potential (28). The membrane potentials were calculated based on the values for Rhodamine 123 fluorescence quenching as determined by the Rhodamine 123 fluorescence in a sample that did not contain mitochondria.

Statistical analysis

Data from the two experimental groups were compared using the Student's t-test. Statistical significance was defined as $P < 0.05$.

Results

Changed ETC enzyme activities and effect of PP in tumour microenvironments in human cancer cells

In hypovascular tumours, both the deprivation of oxygen and glucose were observed, because of the limitation of the blood supply to the tumour tissues. We wondered whether human cancer cells survive under hypoxia–hypoglycemic conditions mimicking tumour microenvironments. Such conditions have been reported in the short term. When HepG2 cells were cultured for 36 h under the depletion of both oxygen and glucose, i.e. hypoxia–hypoglycemic conditions, cells survived whereas they died under glucose starvation in normoxia (29). To confirm cancer cells can survive under microenvironments mimicking tumour conditions in the long term, cells were cultured in glucose-depleted medium under hypoxic conditions for 1 week. In DLD-1, under hypoxia–hypoglycemic conditions, 73.8% cells survived for 7 days (Fig. 2).
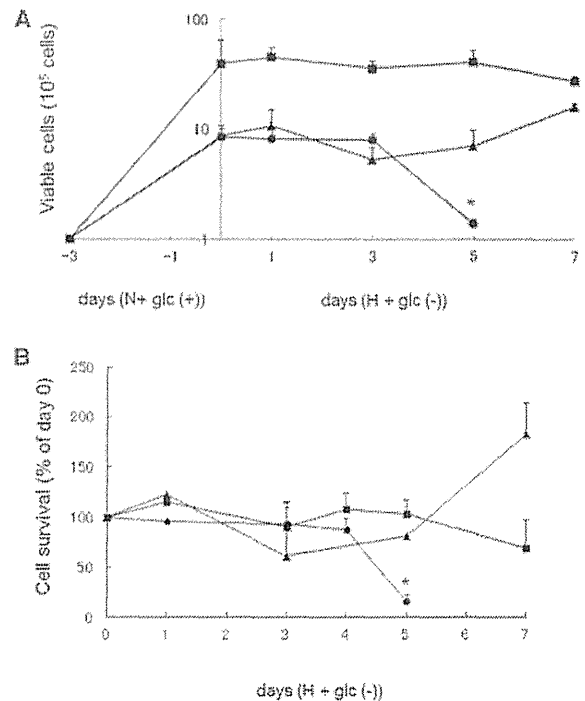

Fig. 2 Cell survivals under hypoxia–hypoglycemic conditions.
(A) Number of surviving cells. (B) The percentages of cell survival from day 0. The circles indicate HDF, the squares indicate DLD-1 and the triangles indicate Panc-1 cultured under 1% O_2 and glucose depleted conditions [H+ glc(−)] for 1–7 days. All the data were expressed as the mean ± SEM of three independent measurements. Statistically significant differences with respect to day 0 are shown by an asterisk (Student's t-test).

Panc-1 also survived under such conditions for 7 days. On the other hand, cell survival rate was decreased in 16.3% of HDF by day 5. Thus, human cancer cells can survive under hypoxia–hypoglycemic conditions for the long term. This result is consistent with the fact that cancer cells in tumour tissues can survive under tumour microenvironments.

In a previous report, activities of the reverse reaction of complex II, which is the component of NADH–FR system, were found in all six human cancer cell lines examined including DLD-1, Panc-1 and HepG2 (20), suggesting that the NADH–FR system can be enabled in cancer cells and NADH–FR activities were detected in all the cell cultures in our experiment (data not shown). Then to examine whether the ETC function changes from normoxic ETC to hypoxic ETC; NADH-oxidase [Fig. 3A(a)] and NADH–FR [Fig. 3A(b)] activities were measured. In DLD-1 cultured under hypoxia–hypoglycemic conditions, NADH-oxidase activity eventually decreased to an undetectable level, whereas NADH–FR activity was 3.0 ± 0.4 nmol/min/mg mitochondrial proteins under normoxia–normoglycemic conditions and 10.4 ± 1.0 nmol/min/mg proteins after 7 days of hypoxia–hypoglycemic conditions [Fig. 3B(a)]. Other cancer cell lines, Panc-1 and HepG2, also showed the same response, i.e. a decrease in NADH-oxidase activity, whereas an increase in NADH–FR activity was
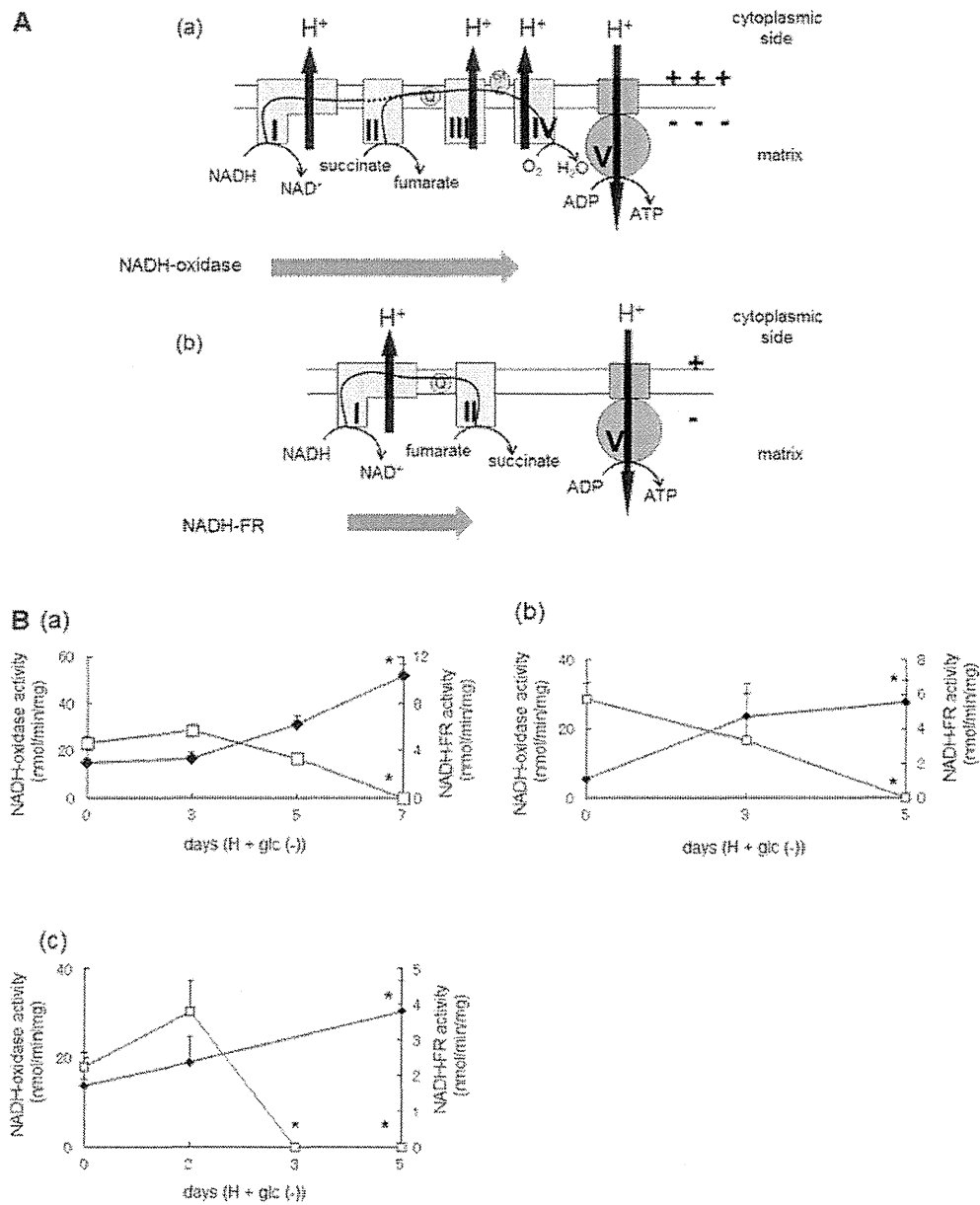
173

Fig. 3 **Electron transport chain enzyme activities in mitochondria.** (A) Mitochondrial respiratory chains. (a) Oxidative phosphorylation system. Under normoxic conditions in mammalian mitochondria, electrons from the TCA cycle pass through complex I (I: NADH–ubiquinone reductase) to ubiquinone (Q), complex III (III: ubiquinol–cytochrome c reductase), cytochrome c (cyt c) and complex IV (IV: cytochrome c oxidase) or through complex II (II: succinate–ubiquinone reductase) to ubiquinone, complex III, cytochrome c and complex IV. At the same time, complex I, complex III and complex IV function as proton pumps to generate a proton gradient, driving complex V (ATP synthase). (b) NADH–FR system. Under hypoxic conditions, electrons pass through complex I and the reverse reaction of complex II (FRD). Only complex I functions as a proton pump, generating a proton gradient and driving complex V even in the absence of oxygen. (B) Mitochondrial ETC enzyme activities from DLD-1 (a), Panc-1 (b) and HepG2 (c) cultured under 1% O_2 and glucose depleted conditions [H+ glc(−)]. The open squares indicate the NADH-oxidase activities (complex I–III–IV). The closed diamonds indicate the NADH–FR activities (complex I–II). All the data were expressed as the mean ± SEM of three independent measurements. Statistically significant differences with respect to day 0 are shown by an asterisk (Student's t-test).

observed under hypoxia–hypoglycemic conditions [Fig. 3B(b,c)]. When the Panc-1 mitochondrial proteins were separated using blue native gel electrophoresis (BN–PAGE), which can separate ETC enzyme complexes according to native forms, the complex I activity per subunit protein (NDUFSA3) was found to remain at almost the same levels under hypoxia–hypoglycemic

conditions [Supplementary Fig. S1C(a)]. However, SDH activities decreased under hypoxia–hypoglycemic conditions and even the iron–sulphur protein (Ip) subunit proteins of complex II were detected at the same levels indicating that protein levels of complex II unchanged under such conditions [Supplementary Figs. S1A(b) and S1B(b)]. Complex

174

IV activities per subunit proteins also decreased under hypoxia–hypoglycemic conditions [Supplementary Fig. S1C(c)]. Moreover, a low molecular weight complex IV subunit, COXI, protein was detected, suggesting the degradation of complex IV [Supplementary Fig. S1B(d)]. These data are consistent with the changes in enzyme activities and the levels of proteins making up the ETC complexes. Complex I changed minimally, both in its activity and its protein level, because complex I contributes to both normoxic and hypoxic ETCs, whereas complexes of normoxic ETC such as complex IV, decreased in their activities and protein levels under conditions mimicking tumour microenvironments.

PP was selectively cytotoxic to human cancer cells cultured in a nutrient-free medium mimicking the tumour microenvironment (10). We investigated whether PP shows cytotoxic effect in human cells, cancer cells and normal cells under normoxia–normoglycemic and hypoxia–hypoglycemic conditions. PP showed a cytotoxic effect for cancer cells, DLD-1 and Panc-1, under hypoxia–hypoglycemic conditions, whereas little cytotoxic effect was observed under normoxia–normoglycemic conditions (Fig. 4). Moreover, PP exerted minimal cytotoxicity on normal fibroblast (HDF) cells under either normoxia–normoglycemic or hypoxia–hypoglycemic conditions (Fig. 4).

Effect of PP on enzyme activities in normoxic and hypoxic ETCs

PP is used as an anthelmintic and is believed to inhibit fumarate respiration in parasitic energy metabolism, although no direct data or evidence has been reported. To confirm the effect of PP on ETC in parasitic and mammalian mitochondria, we measured the enzyme activities of ETC enzymes in adult *A. suum* and bovine heart mitochondria. The activities of hypoxic ETC enzymes such as NADH–FR, NADH–RQR and

QFR, all of which are components of the NADH–FR system, were higher in adult *A. suum* mitochondria than in bovine mitochondria (Table I). These results were consistent with the conclusion that adult *A. suum* uses the NADH–FR system for hypoxic energy metabolism. PP inhibited NADH–RQR, NADH–UQR (complex I) and QFR (complex II) activities, with an IC_{50} of 0.3 µM for NADH–RQR, 33 µM for NADH–UQR and 9.5 µM for QFR in adult *A. suum* mitochondria. For NADH–FR, which is defined as hypoxic complex I and complex II activities, the IC_{50} was 0.5 µM in *A. suum*. The complex II activities, SQR and SDH, both decreased with 50 µM of PP and 50 µM of PA to the same levels in *A. suum* mitochondria. These data suggest that the inhibitory effects on SQR and SDH in *A. suum* were caused by PA and not pyrvinium itself. The minimal side effects of PP are reportedly due to the non-absorption of PP by the gastrointestinal tract in humans (12). However, another pyrvinium salt, pyrvinium chloride. has been reported to be selectively toxic in rodents because of its absorption only in rodent species (30). These reports indicate that the salt types of PP have different effects in mammals.

In bovine heart mitochondria, PP inhibited the NADH–UQR (complex I) and the IC_{50} was 0.7 µM (Table I). PP inhibited QFR in bovine heart mitochondria and the IC_{50} was 14 µM (similar to the level for QFR in *A. suum*), but no inhibitory effects on SQR and SDH were seen. Of note, incubation with 50 µM of PP increased the SQR activity by approximately 150%, whereas PA had no effect on the SQR or SDH activities. These effects of PP on SQR were quite different between *A. suum* and bovine mitochondria.

To confirm the effects of PP on the mammalian ETC overall, the oxygen consumption by bovine mitochondria was measured. As shown in Fig. 5, the reaction started by the addition of succinate, representing the succinate oxidase activity, gradually increased
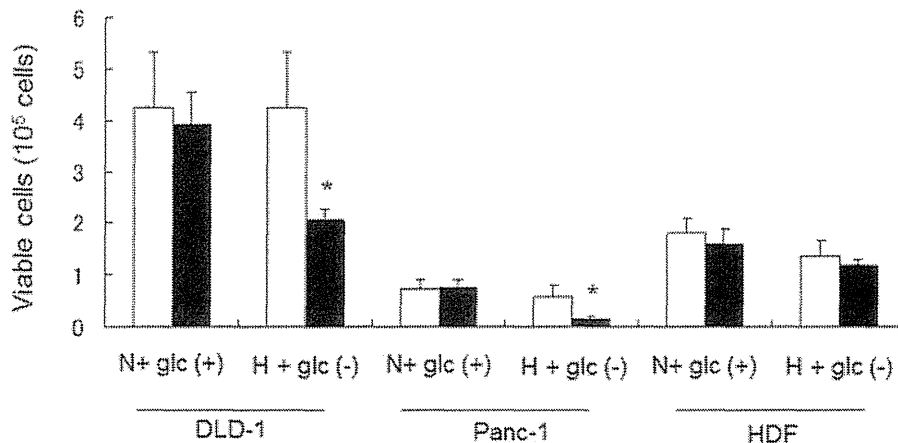
Fig. 4 Cytotoxicity of pyrvinium pamoate in DLD-1, Panc-1 and HDF under normoxia–normoglycemic and hypoxia–hypoglycemic conditions. Cells were cultured in normoglycemic medium at atmospheric oxygen tension [N+ glc(+)] for 3 days and treated with PP (0.1 µM) in N+ glc(+) or glucose-free medium under 1% oxygen [H+ gluc(−)] for 24 h. The open bars indicate the number of viable cells after treatment with DMSO, whereas the closed bars indicate the number of viable cells after treatment with PP. The values reported represent the mean ± SEM of three independent measurements. Statistically significant differences with respect to the control (DMSO treated) are shown by an asterisk (Student's *t*-test).

Table I. Enzyme activities of electron transport chain enzymes and the effects of pyrvinium pamoate and pamoic acid.

	Enzyme activity (nmol/min mg protein)	PP IC$_{50}$ (μM)	Residual activity of 50 μM PP (%)	Residual activity of 50 μM PA (%)
Adult *Ascaris suum* mitochondria				
Complex I+II (NADH–FR)	51.7±8.3	0.5	n.d.	99.4
Complex I (NADH–UQR)	110.3±7.4	33.0	n.d.	102.4
Complex I (NADH–RQR)	65.0±1.7	0.3	n.d.	107.8
Complex II (QFR)	42.2±5.4	9.5	n.d.	105.3
Complex II (SQR)	268.7±24.4	No inhibition	61.7	47.9
Complex II (SDH)	182.4±2.1	No inhibition	59.9	69.5
Bovine heart submitochondrial particles				
Complex I+II (NADH–FR)	8.5±1.9	0.5	n.d.	94.8
Complex I (NADH–UQR)	139.5±33.5	0.7	n.d.	93.3
Complex I (NADH–RQR)	13.4±1.7	2.9	n.d.	n.d.
Complex II (QFR)	6.6±0.3	14.0	n.d.	n.d.
Complex II (SQR)	65.3±10.1	No inhibition	154.2	93.9
Complex II (SDH)	37.2±12.3	No inhibition	100.0	93.0

NADH–FR, NADH–fumarate reductase; NADH–UQR, NADH–ubiquinone reductase; NADH–RQR, NADH–rhodoquinone reductase; QFR, Rhodoquinol–fumarate reductase; SQR, succinate–ubiquinone reductase; SDH, succinate dehydrogenase. n.d., not done.
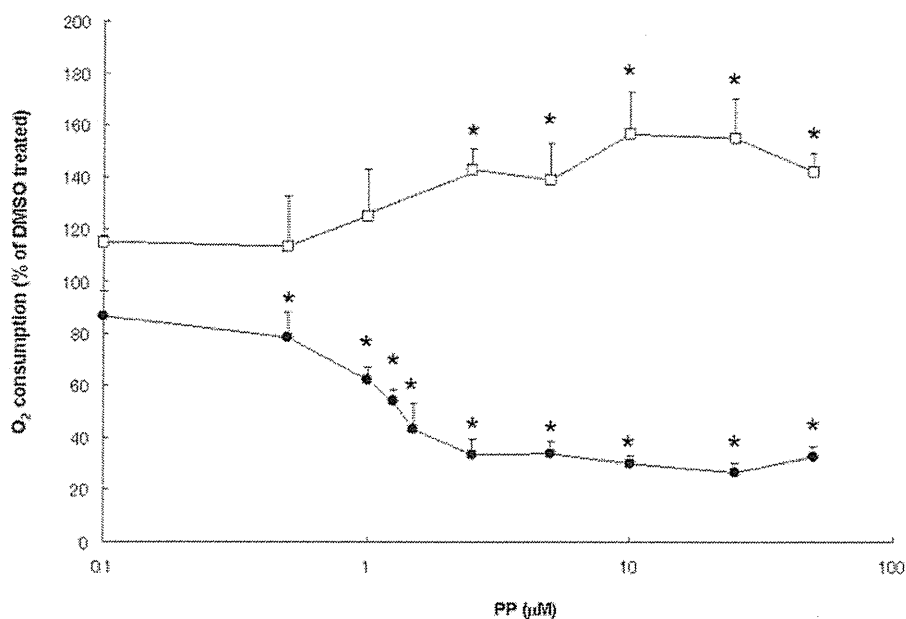
Fig. 5 Effects of pyrvinium pamoate on oxygen consumption in bovine mitochondria. The open squares indicate the percentages of residual activity using succinate as the substrate and the closed circles indicate the percentages of residual activity using NADH as the substrate. The oxygen consumption rate without PP was defined as 100%. The values reported represent the mean ± SEM of three independent measurements. Statistically significant differences with respect to the control (DMSO treated) are shown by an asterisk (Student's *t*-test).

with the addition of PP, whereas the reaction started by the addition of NADH, representing the NADH-oxidase activity, decreased, although the activity remained at 20% for a high dose of PP. These data are consistent with the data in Table I, showing an increase in SQR activity and the partial inhibition of NADH–UQR activity.

Effect of PP on normoxic and hypoxic ETC enzymes and on mitochondrial functions under hypoxia–hypoglycemic conditions

PP inhibited the enzymatic activities in the NADH–FR system in mammalian mitochondria but did not inhibit SQR or SDH, as shown in Table I.

These observations implied that PP has different effects on the ETC enzymes of cancer cells under hypoxia–hypoglycemic conditions, compared with under normoxia–normoglycemic conditions. To confirm whether PP exerts different effects on SQR and NADH–FR activities in cancer cells in tumour microenvironments, we measured these activities in mitochondria from cancer cells cultured under hypoxia–hypoglycemic conditions for 3 and 5 days (7 days in DLD-1). Under normoxia–normoglycemic conditions on day 0, PP increased the SQR activity in both Panc-1 and DLD-1 mitochondria as well as in bovine mitochondria (Fig. 6A). However, after the cells had been cultured under hypoxia–hypoglycemic
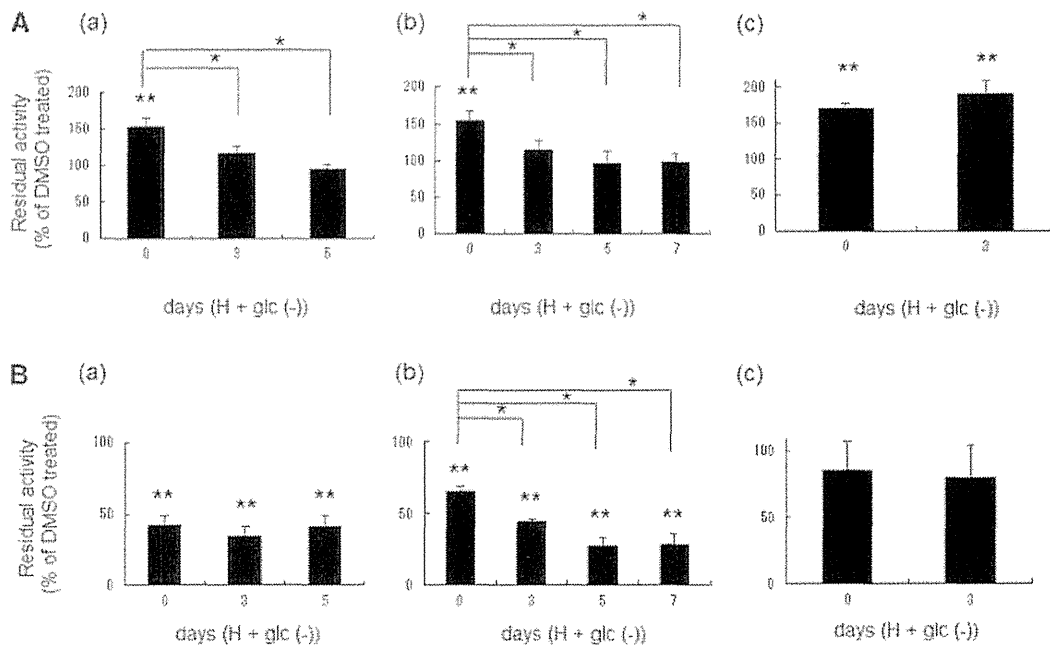
Fig. 6 Effects of pyrvinium pamoate on SQR and NADH–FR activities under hypoxia–hypoglycemic conditions. (A) Effect of 25 µM PP on SQR activity. The percentages of the residual SQR activities from the addition of DMSO instead of PP in mitochondria separated from Panc-1 (a), DLD-1 (b) and HDF (c) cultured under normoxia–normoglycemic conditions [N+ glc (+)] (day 0) and cultured in glucose-free medium under 1% O₂ [H+ glc (−)] [days 3 and 5 (and 7 in DLD-1)] are shown. (B) Effect of 5 µM PP on NADH–FR activity. The percentages of the residual NADH–FR activities in mitochondria separated from Panc-1 (a), DLD-1 (b) and HDF (c) cultured under N+ glc (+) (day 0) and cultured under H+ glc(−) [days 3 and 5 (and 7 in DLD-1)] are shown. The values reported represent the mean ± SEM of three independent measurements. Statistically significant differences are shown by the asterisks ($*P<0.05$ versus day 0, $**P<0.05$ versus DMSO treated, Student's t-test).

conditions for 3–5 days (7 days in DLD-1), PP no longer had any activation effect on SQR [Fig. 6A(a,b)]. When HDF was cultured under the same hypoxic–hypoglycemic conditions, PP increased the SQR activity in a manner similar to that under normoxia–normoglycemic conditions [Fig. 6A(c)]. On the other hand, the NADH–FR activities in Panc-1 and DLD-1 mitochondria were inhibited by PP under both conditions, but an inhibitory effect was not evident in HDF, partly because of the low NADH–FR activity of HDF [Fig. 6B(c)]. Interestingly, in DLD-1, the inhibitory effect on NADH–FR activity gradually increased over time when the cells were cultured under hypoxia–hypoglycemic conditions [Fig. 6B(b)]. PP also inhibited NADH–UQR activity as shown in Table 1 and the effect of PP on NADH–UQR in mitochondria from cultured cells was also compared (Supplementary Fig. S2). PP inhibited NADH–UQR activities under both normoxia–normoglycemic and hypoxia–hypoglycemic conditions in all cell lines including HDF, but the inhibitory effect in HDF was smaller than that in other cancer cell lines. In mitochondria prepared from cancer cells cultured under hypoxia–hypoglycemic conditions, the increase in SQR activity induced by PP disappeared, whereas the reverse reaction of complex II in the NADH–FR system was inhibited by PP. In contrast, under both normoxia–normoglycemic and hypoxia–hypoglycemic conditions, minimal differences in the inhibitory effects of NADH–UQR were observed. The distinct effects of PP on complex II

activities may be one of the reasons why PP is only cytotoxic in cancer cells within tumour microenvironments but does not exhibit cytotoxicity in normal cells or cancer cells within normoxia–normoglycemic environments.

As PP affected both normoxic and hypoxic ETC in mitochondria, we examined the effects of PP on the mitochondrial membrane potential ($\Delta\Psi$m) to confirm how PP affects mitochondrial functions in cancer cells. In normoxic ETC, electrons from the TCA cycle pass via complex I (NADH–UQR) → complex III (ubiquinol–cytochrome c reductase) → complex IV (cytochrome c oxidase) or via complex II (SQR) → complex III → complex IV. Complex I, complex III and complex IV function as proton pumps and generate a proton gradient, which is the driving force for ATP synthesis by complex V (ATP synthase) as shown in Fig. 3A(a). On the other hand, the NADH–FR system is only composed of complex I and the reverse reaction of complex II; thus, only complex I functions as a proton pump, forming a transmembrane electrochemical proton gradient for ATP synthesis through complex V [Fig. 3A(b)]. The generation of a $\Delta\Psi$m indicates that the ETC enzymes are actively functioning as proton pumps. If PP affects the $\Delta\Psi$m, the generation of ATP will be influenced. To understand whether and how the NADH–FR system can generate a $\Delta\Psi$m, fumarate was first used as the substrate of the NADH–FR system and the generation of a $\Delta\Psi$m in mitochondria prepared from cancer cells cultured under

177

normoxia–normoglycemic or hypoxia–hypoglycemic conditions was measured. Because a $\Delta\Psi m$ was generated using the NADH–FR system and both fumarate and NADH as substrates, fumarate was used as a substrate for the generation of $\Delta\Psi m$ in the presence of endogenous NADH. When mitochondria prepared from cells cultured under normoxia–normoglycemic conditions were used, as shown in Fig. 7A(a), $\Delta\Psi m$ was increased by the addition of succinate. The $\Delta\Psi m$ generated by succinate was inhibited by 0.1 mM of cyanide [Fig. 7A(a)]. Cyanide did not inhibit the $\Delta\Psi m$ generated by fumarate, as shown in Fig. 7A(b). As the NADH–FR system is composed of complex I and complex II, and complex IV is not included in this system, the finding that the $\Delta\Psi m$ generated by fumarate was insensitive to cyanide is consistent with the idea that cancer cells utilize the NADH–FR system. As shown in Fig. 7B and C, 0.5 μM of PP inhibited the $\Delta\Psi m$ generated by fumarate in Panc-1 and DLD-1. No inhibitory effect of PP was observed on the $\Delta\Psi m$ generated by succinate in Panc-1 [Fig. 7B(a)]. Moreover, in DLD-1, PP slightly but reproducibly increased the $\Delta\Psi m$ generated by succinate [Fig. 7C(c)]. A similar effect of PP on the $\Delta\Psi m$ generated by succinate was observed in HepG2 cells (data not shown). These data coincided with the data in Fig. 6 and PP increased the activity of SQR under normoxia–normoglycemic conditions.

Effect of PP on the Fp subunit in complex II

As PP increased the activity of SQR (Table I, Figs 5 and 6), the effect of PP on human complex II was examined. Previously, we reported that the enzyme activities of human complex II are regulated by the phosphorylation of the flavoprotein (Fp) subunit, which is the catalytic subunit of complex II (*20*). In our previous paper, treatment with a phosphatase caused the dephosphorylation of the Fp subunit and an increase in the SQR activity, whereas the reverse reaction of complex II, *i.e.* fumarate reductase (FRD) activity were decreased in DLD-1 mitochondria. In contrast, treatment with protein kinase caused the phosphorylation of the Fp subunit and a decrease in SQR activity with a concomitant increase in FRD activity. As mentioned, treatment with PP resulted in an increase in SQR activity and we suspected that PP treatment may modulate the phosphorylation of the Fp subunit of complex II. In Fig. 8A, treatment with phosphatase increased the SQR activity in DLD-1 mitochondria and PP also increased the SQR activity, relative to a control (0 U of Antarctic phosphatase treatment). Moreover, treatment with PP plus phosphatase exerted a stronger activation effect on SQR. However, 2 U of phosphatase treatment produced the same activation effect as PP plus phosphatase, suggesting that a high amount of phosphatase can cause the complete dephosphorylation of the Fp subunit related to SQR activity. Therefore, PP has the same effect as phosphatase on SQR activity.

Next, to determine whether PP causes the dephosphorylation of the Fp subunit in a manner similar to phosphatase treatment, the phosphorylation status of the Fp subunit was examined. In Fig. 8B, Fp protein

spots with different pI values were detected and the spot intensities differed for each treatment. The ratios of the intensity of spot No.3 to the intensity of spot No.4 were increased after PP treatment, indicating that the ratio of dephosphorylated Fp proteins increased (Fig. 8C). These data suggest that PP causes the dephosphorylation of Fp leading to an increase in SQR activity and the effect of PP might be related to mitochondrial phosphatases. To address the question of whether the effect of PP arises from the activation of phosphatase, PP was treated with phosphatase inhibitors. In Fig. 9A, PP increased the SQR activity, whereas treatment with PP and phosphatase inhibitors did not produce any increase in SQR activity. Similarly, the treatment with phosphatase increased the SQR activity, whereas the treatment with phosphatase together with phosphatase inhibitors did not increase the SQR activity (Fig. 9B). These data suggest that PP affects the complex II activity indirectly, indicating that PP enhances SQR activity through the activation of mitochondrial phosphatase(s).

Discussion

In this report, we investigated the existence and function of the hypoxic ETC, the NADH–FR system, in tumour microenvironments in human cancer cells and the mechanisms of the effects of PP on parasitic and mammalian ETC enzymes. PP inhibited the hypoxic ETC, NADH–FR system in both parasitic and mammalian mitochondria, showing that the NADH–FR system is active in both parasitic and mammalian mitochondria. Moreover, PP inhibited SQR activity in parasitic mitochondria but activated SQR activity in mammalian mitochondria. The species-specific effect of PP is likely caused by the distinct function of complex II in mammalian mitochondria. We also showed that PP had different effects on complex II activities in cancer cells cultured under normoxic–normoglycemic conditions and under hypoxic–hypoglycemic conditions, suggesting that treatment with PP may be selectively effective against cancer cells in tumour microenvironments. In addition, we showed that PP dephosphorylated the Fp subunit in complex II and activated SQR activity, similar to the effect of phosphatase, indicating that PP activates mitochondrial protein phosphatases that maintain the functions of ETCs.

Recently, PP has been shown to exert not only anti-pinworm but also anti-malarial and anti-cryptosporidium activities (*14, 15*). The search for anti-parasitic drugs is continuing in the 21st century and pathways of parasitic energy metabolism, such as the NADH–FR system, are gradually becoming viewed as important candidate targets for anti-parasitic drugs (*31, 32*). In our study we found that PP inhibited the NADH–FR system, consisting of both complex I and complex II activities, in *A. suum* mitochondria, suggesting that PP kills these parasites by inhibiting the NADH–FR system. Therefore, this system may be important for energy production in parasites and may be a useful target
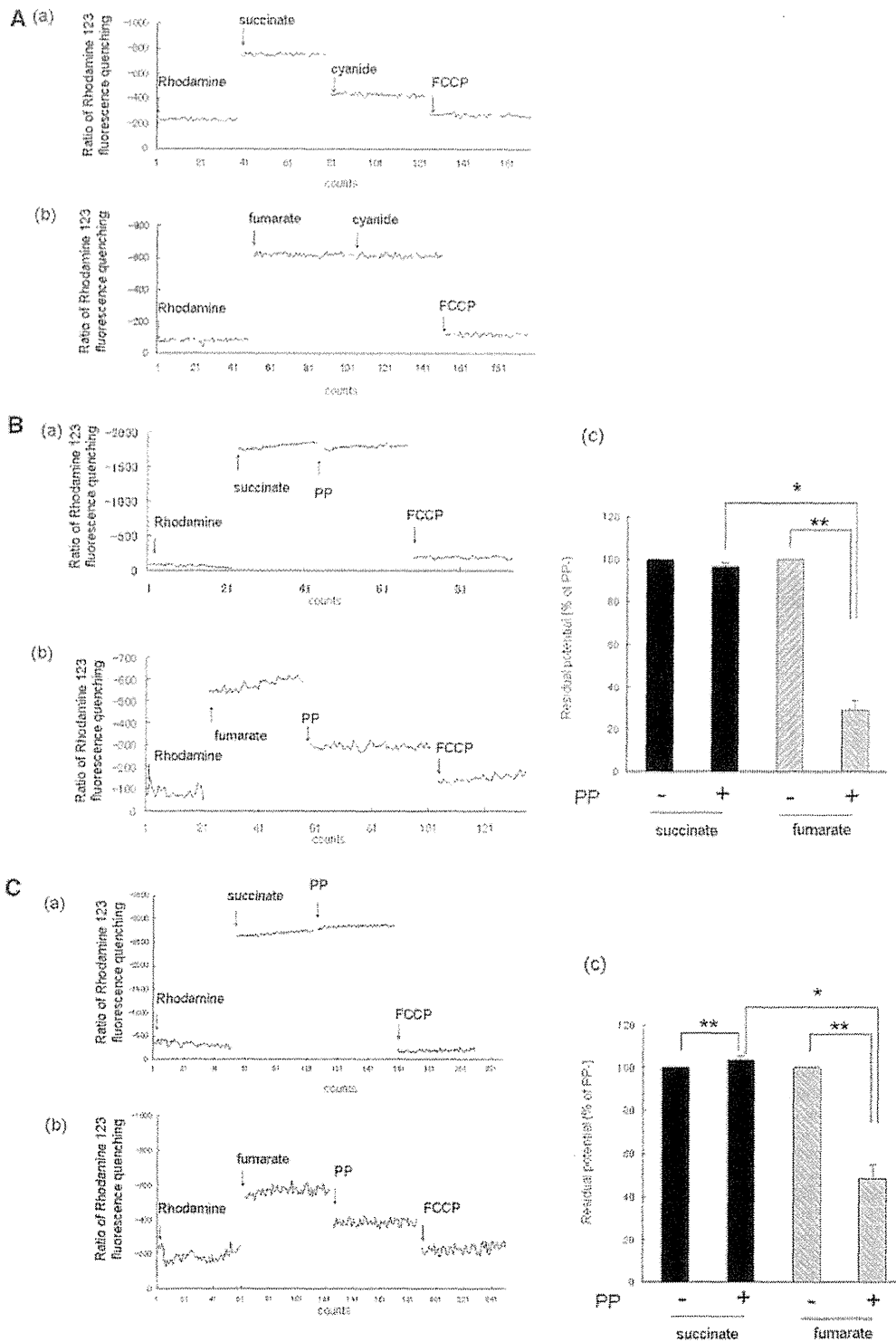
Fig. 7 **Effect of pyrvinium pamoate on mitochondrial membrane potentials.** (A) Effect of 0.1 mM cyanide on the $\Delta\Psi m$ in Panc-1 mitochondria. The values of Rhodamine 123 fluorescence quenching after the addition of succinate in mitochondria from Panc-1 cultured under normoxia—normoglycemic conditions [N+ glc(+)] (a) or after the addition of fumarate in mitochondria from Panc-1 cultured with glucose-free medium under 1% O_2 [H+ glc(−)] for 5 days (b) are shown. (B) Effect of 0.5 μM PP on the $\Delta\Psi m$ in Panc-1 mitochondria. The values of Rhodamine 123 fluorescence quenching starting after the addition of succinate in mitochondria from Panc-1 cultured under N+ glc(+) (a) or after the addition of fumarate in mitochondria from Panc-1 cultured under H+ glc(−) for 5 days (b) are shown. The percentages of the residual $\Delta\Psi m$ in mitochondria from Panc-1 cultured under N+ glc(+) (succinate as substrate) and cultured under H+ glc(−) for 5 days (fumarate as substrate) are also shown (c). (C) Effect of 0.5 μM PP on the $\Delta\Psi m$ in DLD-1 mitochondria. The values of Rhodamine 123 fluorescence quenching after the addition of succinate in mitochondria from DLD-1 cultured under N+ glc(+) (a) or after the addition of fumarate in mitochondria from DLD-1 cultured under H+ glc(−) for 7 days (b) are shown. The percentages of the residual $\Delta\Psi m$ in mitochondria from DLD-1 cultured under the N+ glc(+) (succinate as substrate) and cultured under H+ glc(−) 7 days (fumarate as substrate) are shown (c). The values reported represent the mean ± SEM of three independent measurements. Statistically significant differences are shown by the asterisks (*$P < 0.05$ succinate versus fumarate. **$P < 0.05$ versus PP −, Student's t-test).

179

A

B   *pI* 5.9   *pI* 7.0

a)
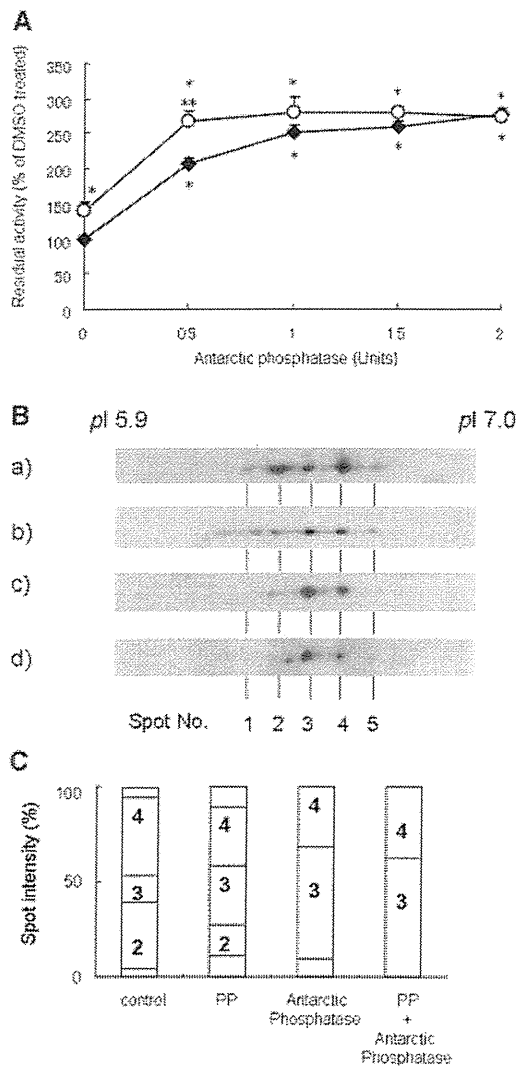
b)

c)

d)

Spot No.   1   2   3   4   5

C

Fig. 8 Effects of pyrvinium pamoate and phosphatase on complex II. (A) Effect of PP and Antarctic Phosphatase on SQR activity. The percentages of the residual SQR activities after the addition of DMSO in solubilized mitochondrial proteins from DLD-1 cultured under normoxia—normoglycemic conditions [N+ glc(+)] and treated with various units of Antarctic Phosphatase and/or treated with 25 µM PP are shown. The closed diamonds indicate treatment with Antarctic phosphatase, whereas the open circles indicate treatment with Antarctic phosphatase plus PP. The values reported represent the mean ± SEM of three independent measurements. Statistically significant differences are shown by the asterisks (*P < 0.05 versus phosphatase −/PP −, **P < 0.05 versus phosphatase +/PP −, Student's *t*-test). (B) Separation and detection of the Fp subunit in solubilized mitochondrial proteins from DLD-1 cultured under N+ glc(+) using 2-D gel electrophoresis. Untreated (a), treated with 25 µM PP for 10 min at 30°C (b) or treated with 0.5 U of Antarctic phosphatase for 2 h at 37°C (c). Treated with 25 µM of PP for 10 min at 30°C and 0.5 U of Antarctic phosphatase for 2 h at 37°C (d). (C) Spot intensities of (B). The numbers show the spot No. of (B).
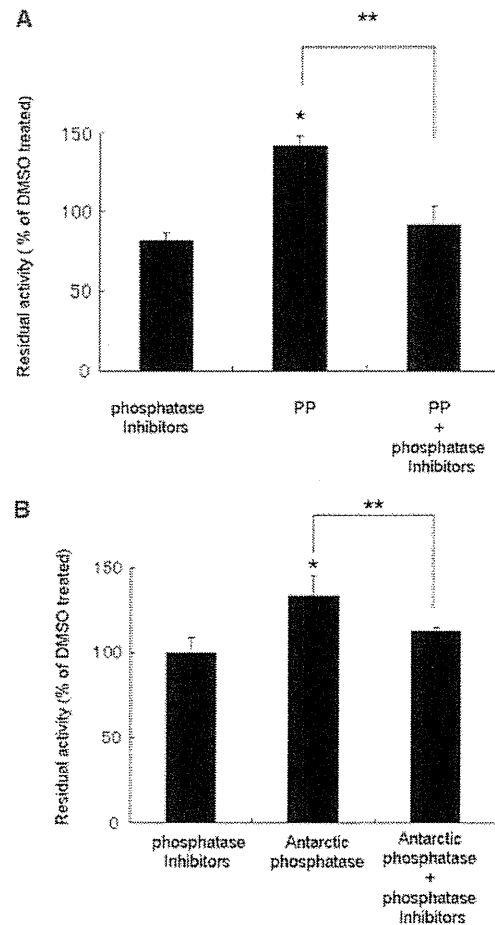
A

B

Fig. 9 Effect of pyrvinium pamoate, phosphatase and phosphatase inhibitors on SQR activity. (A) Percentages of residual SQR activities after the addition of DMSO in solubilized mitochondrial proteins from DLD-1 cultured under normoxia—normoglycemic conditions [N+ glc(+)] and treatment with a phosphatase inhibitor cocktail and/or 25 µM PP for 10 min at 30°C. Statistically significant differences are shown by the asterisks (*P < 0.05 versus DMSO treated, **P < 0.05 phosphatase inhibitors −/PP + versus phosphatase inhibitors +/PP +, Student's *t*-test). (B) Percentages of residual SQR activities after the addition of DMSO in solubilized mitochondrial proteins from DLD-1 cultured under N+ glc(+) and treatment with a phosphatase inhibitor cocktail, 0.5 U of Antarctic phosphatase or 0.5 U of Antarctic phosphatase plus a phosphatase inhibitor cocktail for 2 h at 37°C. The values reported represent the mean ± SEM of three independent measurements. Statistically significant differences are shown by the asterisks (*P < 0.05 versus DMSO treated, **P < 0.05 phosphatase inhibitors −/Antarctic phosphatase + versus phosphatase inhibitors +/Antarctic phosphatase +, Student's *t*-test).

for anti-parasitic drugs. How PP exerts species-specific effects between parasites and hosts needs to be understood. In our study, PP exerted different effects on complex II in parasites and mammals, with PP inhibiting complex II activities in both the normoxic ETC and the NADH—FR system in parasites and increasing

SQR activity in mammals. Complex II in *A. suum* has been well characterized and complex II (SQR) and complex II (QFR) contain different Fp and the small cytochrome *b* (CybS) subunits (33, 34). On the other hand, modification of the Fp subunit in mammalian complex II switches its function from SQR to FRD (20). Therefore, one of the species-specific effects of PP is caused by its different effects on complex II in parasitic and mammalian mitochondria, which have different complex II characteristics.

To consider the side effects of PP, the effects of PP on mammalian ETCs should be compared in both

cancer cells and normal cells and under an ordinary environment and tumour microenvironments. In mammalian mitochondria, we showed that PP inhibited NADH–FR activity, but the activity was low in bovine mitochondria and cancer cell lines, such as DLD-1 (35), compared with *A. suum* mitochondria. Moreover, SQR activity was increased by PP in bovine mitochondria and human cancers and in the mitochondria of normal cells under normoxia–normoglycemic conditions. In addition, PP did not inhibit the $\Delta\Psi m$ generated by normoxic ETC starting with complex II. These data suggest that PP does not interfere with ATP synthesis via normoxic mitochondrial ETC through complex II, even when complex I is partially inhibited and is unlikely to produce severe side effects in normal human tissues. Moreover, PP exerted an anticancer effect, inhibiting tumour formation in xenografts (10) and PP inhibited hypoxic ETC under tumour microenvironmental conditions in the present study. Therefore, PP has a minimal cytotoxicity in normal cells but is effective against cancer cells under tumour microenvironmental conditions and PP may serve as a good anticancer compound with minimal side effects.

To understand why PP is cytotoxic only in tumour microenvironments, we examined the NADH–FR system, a unique energy metabolic pathway, under hypoglycemic and hypoxic conditions. When glucose is limited, amino acids can be used for energy production instead of glucose, *e.g.* aspartate → oxaloacetate → malate → fumarate (36) and fumarate is the substrate of the NADH–FR system. Despite the limited glucose concentrations in tumour tissues in tumour microenvironments, the accumulation of amino acids has been observed in tumour tissues (3, 37). One of the reasons for the accumulation of amino acids is thought to be the activation of the autophagic degradation of proteins under nutrient-starved conditions (38). The NADH–FR system is only composed of complex I and the reverse reaction of complex II; this system results in succinate formation via the fumarate reductase activity in complex II (35). This system does not need oxygen, allowing it to function under hypoxic conditions. The final product in this system, succinate, is known to have an important role in the hypoxic response. Succinate inhibits prolyl hydroxylase (PHD), leading to the stabilization of hypoxia inducible factor (HIF) −1α degradation (39). As HIF is a major regulator of the hypoxic response, the NADH–FR system may have an important role in the activation of a pseudo-hypoxic pathway.

We showed that PP inhibited the $\Delta\Psi m$ generated by fumarate, which is a substrate of the NADH–FR system. In contrast, PP did not inhibit the $\Delta\Psi m$ generated by succinate; moreover, a slight activation effect was observed in DLD-1 and HepG2. The $\Delta\Psi m$ generated by fumarate was not inhibited by cyanide, consistent with the action of the NADH–FR system. In this system, complex I functions as a proton pump to form a transmembrane electrochemical proton gradient, the driving force in ATP synthesis. Therefore, the NADH–FR system may be involved in ATP generation under tumour microenvironmental conditions

and PP may interfere with ATP synthesis by inhibiting the NADH–FR system in cancer cells in tumour microenvironments. Moreover, the $\Delta\Psi m$ is an important factor in the maintenance of mitochondria. The phosphatase and tensin homolog deleted on chromosome 10 (PTEN)-induced putative kinase 1 (PINK1) and Parkin reportedly play important roles in the quality control of mitochondria through the clearance of damaged mitochondria via autophagy; after the loss of the $\Delta\Psi m$, PINK1 recruits Parkin into mitochondria and promotes mitophagy in *Drosophila* and both neurogenic and non-neurogenic human cells (40–42). Therefore, the generation of $\Delta\Psi m$ by the NADH–FR system in tumour microenvironments likely has important roles in ATP generation and the maintenance of mitochondrial quality.

PP increased the SQR activity in the mitochondria of cancer cells cultured under normoxia–normoglycemic conditions; however, SQR was not activated in cancer cells cultured under hypoxia–hypoglycemic conditions. These observations raise two questions: how does PP affect complex II and how does complex II differ under normal and tumour microenvironmental conditions? Post-translational modifications in mitochondrial proteins, such as phosphorylation and acetylation, have been identified and some of these modifications regulate mitochondrial functions (43, 44). In complex II, the acetylation of the Fp subunit has been reported and the deacetylase Sirtuin 3 deacetylates the Fp subunit (45, 46). The phosphorylation of the Fp subunit has also been shown and we previously reported that the phosphorylation of the Fp changed its activity, with the activity of SQR increasing when Fp was dephosphorylated and the activity of FRD increasing when Fp was phosphorylated. Under tumour microenvironmental conditions, the phosphorylated form of Fp and FRD activity concomitantly increased, whereas the dephosphorylated form of Fp and SQR activity decreased (20). Treatment of the cells with PP resulted in the dephosphorylation of the Fp subunit, which might have been mediated by the activation of mitochondrial phosphatase(s). However, several protein kinases and phosphatases have been detected in mitochondria, although the details of their physiological roles are poorly understood (47). Regarding complex II, Salvi *et al.* (48) reported that Fgr tyrosine kinase, which is a member of the Src kinase family, phosphorylated the Fp subunit, but little information on Fgr tyrosine kinase is available. Therefore, a direct target of PP, which activates SQR, could not be found at present. PP has also been shown to inhibit the phosphorylation of PKB/Akt under hypoglycemic condition (10). The inhibition of the PKB/Akt pathway may be involved in cytotoxicity, specifically under hypoglycemic condition, but the inhibition of the PKB/Akt pathway by wortmannin and LY294002 did not cause selective cytotoxicity under hypoglycemic condition (49). These data suggest the importance of the PKB/Akt pathway in selective cytotoxicity under hypoglycemic condition even though this pathway is not a direct target of PP. Although the direct target of PP remains

unknown, the key effects of PP such as its anticancer and selective cytotoxic effects, may arise through the inhibition of the NADH–FR system. Therefore, the NADH–FR system is a good target for anticancer therapy.

In this report, we showed that PP affects mitochondrial energy metabolism through the inhibition/activation of ETC enzymes. Therefore, the NADH–FR system is a novel mitochondrial pathway for energy metabolism in tumour microenvironments and PP is a promising leading compound for the development of tumour-microenvironment-specific anticancer agents.

Supplementary Data

Supplementary data are available at *JB* Online.

Acknowledgements

Conflict of interest

None declared.

References

1. Brown, J.M. and Wilson, W.R. (2004) Exploiting tumour hypoxia in cancer treatment. *Nat. Rev. Cancer* **4**, 437–447

2. Vaupel, P., Kallinowski, F., and Okunieff, P. (1989) Blood flow, oxygen and nutrient supply, and metabolic microenvironment of human tumors: a review. *Cancer Res.* **49**, 6449–6465

3. Hirayama, A., Kami, K., Sugimoto, M., Sugawara, M., Toki, N., Onozuka, H., Kinoshita, T., Saito, N., Ochiai, A., Tomida, M., Esumi, H., and Soga, T. (2009) Quantitative metabolome profiling of colon and stomach cancer microenvironment by capillary electrophoresis time-of-flight mass spectrometry. *Cancer Res.* **69**, 4918–4925

4. Warburg, O. (1956) On respiratory impairment in cancer cells. *Science* **124**, 269–270

5. Zu, X.L. and Guppy, M. (2004) Cancer metabolism: facts, fantasy, and fiction. *Biochem. Biophys. Res. Comm.* **313**, 459–465

6. Lu, L., Kunimoto, S., Yamazaki, Y., Kaminishi, M., and Esumi, H. (2004) Kigamicin D, a novel anticancer agent based on a new anti-austerity strategy targeting cancer cells' tolerance to nutrient starvation. *Cancer Sci.* **95**, 547–552

7. Teicher, B.A., Lazo, J.S., and Sartorelli, A.C. (1981) Classification of antineoplastic agents by their selective toxicities toward oxygenated and hypoxic tumor cells. *Cancer Res.* **41**, 73–81

8. Onozuka, H., Tsuchihara, K., and Esumi, H. (2011) Hypoglycemic/hypoxic condition in vitro mimicking the tumor microenvironment markedly reduced the efficacy of anticancer drugs. *Cancer Sci.* **102**, 975–982

9. Awale, S., Lu, J., Kalauni, S.K., Kurashima, Y., Tezuka, Y., Kadota, S., and Esumi, H. (2006) Identification of arctigenin as an antitumor agent having the ability to eliminate the tolerance of cancer cells to nutrient starvation. *Cancer Res.* **66**, 1751–1757

10. Esumi, H., Lu, J., Kurashima, Y., and Hanaoka, T. (2004) Antitumor activity of pyrvinium pamoate, 6-(dimethylamino)-2-[2-(2,5-dimethyl-1-phenyl-1H-pyrrol-3-yl)ethenyl]-1-methyl-quinolinium pamoate salt, showing preferential cytotoxicity during glucose starvation. *Cancer Sci* **95**, 685–690

11. Kita, K., Nihei, C., and Tomitsuka, E. (2003) Parasite mitochondria as drug target: Diversity and dynamic changes during the life cycle. *Curr. Med. Chem.* **10**, 2535–2548

12. Buchanan, R.A., Barrow, W.B., Heffelfinger, J.C., Kinkel, A.W., Smith, T.C., and Turner, J.L. (1974) Pyrvinium pamoate. *Clin. Pharmacol. Ther.* **16**, 716–719

13. Sheth, U.K. (1975) Mechanisms of anthelmintic action. *Prog. Drug Res.* **19**, 147–157

14. Downey, A.S., Chong, C.R., Graczyk, T.K., and Sullivan, D.J. (2008) Efficacy of pyrvinium pamoate against *Cryptosporidium parvum* infection in vitro and in a neonatal mouse model. *Antimicrob. Agents Chemother.* **52**, 3106–3112

15. Chong, C.R., Chen, X., Shi, L., Liu, J.O., and Sullivan, D.J.J. (2006) A clinical drug library screen identifies astemizole as an antimalarial agent. *Nat. Chem. Biol.* **2**, 415–416

16. Yu, D.H., Macdonald, J., Liu, G., Lee, A.S., Ly, M., Davis, T., Ke, N., Zhou, D., Wong-Staal, F., and Li, Q.X. (2008) Pyrvinium targets the unfolded protein response to hypoglycemia and its anti-tumor activity is enhanced by combination therapy. *PLoS One* **3**, e3951

17. Saito, S., Furuno, A., Sakurai, J., Sakamoto, A., Park, H.R., Shin-Ya, K., Tsuruo, T., and Tomida, A. (2009) Chemical genomics identifies the unfolded protein response as a target for selective cancer cell killing during glucose deprivation. *Cancer Res.* **15**, 4225–4234

18. Jones, J.O., Bolton, E.C., Huang, Y., Feau, C., Guy, R.K., Yamamoto, K.R., Hann, B., and Diamond, M.I. (2009) Non-competitive androgen receptor inhibition *in vitro* and *in vivo*. *Proc. Natl. Acad. Sci. USA* **106**, 7233–7238

19. Sakamoto, K., Nomura, K., and Miyoshi, H (2002) Synthesis and electron transfer activity of azido ubiquinone-2. *J. Pestic. Sci.* **27**, 147–149

20. Tomitsuka, E., Kita, K., and Esumi, H. (2009) Regulation of succinate-ubiquinone reductase and fumarate reductase activities in complex II by phosphorylation of its flavoprotein subunit. *Proc. Jpn. Acad. Ser. B* **85**, 258–265

21. Yamashita, T., Inoue, T., Miyoshi, H., Sakamoto, K., Osanai, A., Nakamaru-Ogiso, E., and Kita, K. (2004) Rhodoquinone reaction site of mitochondrial complex I, in parasitic helminth, *Ascaris suum*. *Biochim. Biophys. Acta* **1608**, 97–103

22. Matsuno-Yagi, A. and Hatefi, Y. (1985) Studies on the mechanism of oxidative phosphorylation. *J. Biol. Chem.* **260**, 14424–14427

23. Bradford, M.M. (1976) A rapid and sensitive method for the quantitation of microgram quantities of protein utilizing the principle of protein-dye binding. *Anal. Biochem.* **72**, 248–254

24. Tomitsuka, E., Goto, Y., Taniwaki, M., and Kita, K. (2003) Direct evidence for expression of Type II flavoprotein subunit in human complex II (succinate-ubiquinone reductase). *Biochem. Biophys. Res. Comm.* **311**, 774–779

25. Miyadera, H., Hiraishi, A., Miyoshi, H., Sakamoto, K., Mineki, R., Murayama, K., Nagashima, K.V.P., Matsuura, K., Kojima, S., and Kita, K. (2003) Complex II from phototrophic purple bacterium *Rhodoferax fermentans* displays rhodoquinol-fumarate reductase activity. *Eur. J. Biochem.* **270**, 1863–1874

26. Omura, S., Miyadera, H., Ui, H., Shiomi, K., Yamaguchi, Y., Masuma, R., Nagamitsu, T., Takano, D., Sunazuka, T., Harder, A., Kolbl, H., Namikoshi, M., Miyoshi, H., Sakamoto, K., and Kita, K. (2001) An anthelmintic compound, nafuredin, shows selective inhibition of complex I in helminth mitochondria. *Proc. Natl. Acad. Sci. USA* **98**, 60–62

27. Trounce, I.A., Kim, Y.L., Jun, A.S., and Wallace, D.C. (1996) Assessment of mitochondrial oxidative phosphorylation in patient muscle biopsies, lymphoblasts and transmitochondrial cell lines. *Methods Enzymol.* **264**, 484–509

28. Esposti, M.D. (2001) Assessing functional integrity of mitochondria *in vitro* and *in vivo*. *Methods Cell Biol.* **65**, 75–96

29. Esumi, H., Izuishi, K., Kato, K., Hashimoto, K., Kurashima, Y., Kishimoto, A., Ogura, T., and Ozawa, T. (2002) Hypoxia and nitric oxide treatment confer tolerance to glucose starvation in a 5'-AMP-activated protein kinase-dependent manner. *J. Biol. Chem.* **277**, 32791–32798

30. Roszkowski, A.P. (1967) Comparative toxicity of rodenticides. *Fed. Proc.* **26**, 1082–1088

31. Kita, K., Shiomi, K., and Omura, S. (2007) Advances in drug discovery and biochemical studies. *Trends Parasitol.* **23**, 223–229

32. Osanai, A., Harada, S., Sakamoto, K., Shimizu, H., Inaoka, D.K., and Kita, K. (2009) Crystallization of mitochondrial rhodoquinol-fumarate reductase from the parasitic nematode *Ascaris suum* with the specific inhibitor flutolanil. *Acta Cryst.* **F65**, 941–944

33. Kita, K. and Takamiya, S. (2002) Electron-transfer complexes in *Ascaris* mitochondria. *Adv. Parasitol.* **51**, 96–131

34. Iwata, F., Shinjyo, N., Amino, H., Sakamoto, K., Islam, M.K., Tsuji, N., and Kita, K. (2008) Change of subunit composition of mitochondrial complex II (succinate-ubiquinone reductase/quinol-fumarate reductase) in *Ascaris suum* during the migration in the experimental hosts. *Parasitol. Int.* **57**, 54–61

35. Tomitsuka, E., Kita, K., and Esumi, H. (2010) New target for anticancer therapy- a novel mitochondrial energy metabolism, the NADH-fumarate reductase system, in tumor microenvironments. *Ann. N.Y. Acad. Sci.* **1201**, 44–49

36. Pisarenko, O., Studneva, I., Khlopkov, V., Solomatina, E., and Ruuge, E. (1988) An assessment of anaerobic metabolism during ischemia and reperfusion in isolated guinea pig heart. *Biochim. Biophys. Acta* **934**, 55–63

37. Denkert, C., Budczies, J., Weichert, W., Wohlgemuth, G., Scholz, M., Kind, T., Niesporek, S., Noske, A., Buckendahl, A., Dietel, M., and Fiehn, O. (2008) Metabolite profiling of human colon carcinoma-deregulation of TCA cycle and amino acid turnover. *Mol. Cancer* **18**, 72

38. Tsuchihara, K., Fujii, S., and Esumi, H. (2008) Autophagy and cancer: dynamism of the metabolism of tumor cells and tissues. *Cancer Lett.* **278**, 130–138

39. Raimundo, N., Baysal, B.E., and Shadel, G.S. (2011) Revisiting the TCA cycle: signaling to tumor formation. *Trends Mol. Med.* **17**, 641–649

40. Ziviani, E., Tao, R.N., and Whitworth, A.J. (2010) *Drosophila* parkin requires PINK1 for mitochondrial translocation and ubiquitinates mitofusin. *Proc. Natl. Acad. Sci. USA* **107**, 5018–5023

41. Narendra, D., Tanaka, A., Suen, D.F., and Youle, R.J. (2008) Parkin is recruited selectively to impaired mitochondria and promotes their autophagy. *J. Cell Biol.* **183**, 795–803

42. Vives-Bauza, C., Zhou, C., Huang, Y., Cui, M., de Vries, R.L.A., Kim, J., May, J., Tocilescu, M.A., Liu, W., Ko, H.S., Magrane, J., Moore, D.L., Dawson, V., Grailhe, R., Dawson, T.M., Li, C., Tieu, K., and Przedborski, S. (2010) PINK1-dependent recruitment of Parkin to mitochondria in mitophagy. *Proc. Natl. Acad. Sci. USA* **107**, 378–383

43. Hopper, R., Carroll, S., Aponte, A.M., Johnson, D.T., French, S., Shen, R.F., Witzmann, F.A., Harris, R.A., and Balaban, R.S. (2006) Mitochondrial matrix phosphoproteome: effect of extra mitochondrial calcium. *Biochemistry* **45**, 2524–2536

44. Zhao, S., Xu, W., Jiang, W., Yu, W., Lin, Y., Zhang, T., Yao, J., Zhou, L., Zeng, Y., Li, H., Li, Y., Shi, J., An, W., Hancock, S.M., He, F., Qin, L., Chin, J., Yang, P., Chen, X., Lei, Q., Xiong, Y., and Guan, K.L. (2010) Regulation of cellular metabolism by protein lysine acetylation. *Science* **327**, 1000–1004

45. Cimen, H., Han, M.J., Yang, Y., Tong, Q., Koc, H., and Koc, E.C. (2010) Regulation of succinate dehydrogenase activity by SIRT3 in mammalian mitochondria. *Biochemistry* **49**, 304–311

46. Finley, L.W., Haas, W., Desquiret-Dumas, V., Wallace, D.C., Procaccio, V., Gygi, S.P., and Haigis, M.C. (2011) Succinate dehydrogenase is a direct target of sirtuin 3 deacetylase activity. *PLoS One* **6**, e23295

47. Pagliarini, D.J. and Dixon, J.E. (2006) Mitochondrial modulation: reversible phosphorylation takes center stage? *Trends Biochem. Sci.* **31**, 26–34

48. Salvi, M., Morrice, N.A., Brunati, A.M., and Toninello, A. (2007) Identification of the flavoprotein of succinate dehydrogenase and aconitase as *in vitro* mitochondrial substrates of Fgr tyrosine kinase. *FEBS Lett.* **581**, 5579–5585

49. Izuishi, K., Kato, K., Ogura, T., Kinoshita, T., and Esumi, H. (2000) Remarkable tolerance of tumor cells to nutrient deprivation: possible new biochemical target for cancer therapy. *Cancer Res.* **60**, 6201–6207

Full Paper

KRAS mutations in primary tumours and post-FOLFOX metastatic lesions in cases of colorectal cancer

Y Kawamoto[1,2,3,4], K Tsuchihara[*,2], T Yoshino[3], N Ogasawara[2], M Kojima[5], M Takahashi[3], A Ochiai[5], H Bando[3], N Fuse[3], M Tahara[3], T Doi[3], H Esumi[2], Y Komatsu[4] and A Ohtsu[3]

[1]Department of Gastroenterology, Hokkaido University Graduate School of Medicine, Sapporo 060-8638, Japan; [2]Cancer Physiology Project, Research Center for Innovative Oncology, National Cancer Center Hospital East, Kashiwa 277-8577, Japan; [3]Department of Gastroenterology and Gastrointestinal Oncology, National Cancer Center Hospital East, Kashiwa 277-8577, Japan; [4]Department of Cancer Center, Hokkaido University Hospital, Sapporo 060-8638, Japan; [5]Pathology Division, Research Center for Innovative Oncology, National Cancer Center Hospital East, Kashiwa 277-8577, Japan

BACKGROUND: KRAS mutations are predictive markers for the efficacy of anti-EGFR antibody therapies in patients with metastatic colorectal cancer. Although the mutational status of KRAS is reportedly highly concordant between primary and metastatic lesions, it is not yet clear whether genotoxic chemotherapies might induce additional mutations.

METHODS: A total of 63 lesions (23 baseline primary, 18 metastatic and 24 post-treatment metastatic) from 21 patients who were treated with FOLFOX as adjuvant therapy for stage III/IV colorectal cancer following curative resection were examined. The DNA samples were obtained from formalin-fixed paraffin-embedded specimens, and KRAS, NRAS, BRAF and PIK3CA mutations were evaluated.

RESULTS: The numbers of primary lesions with wild-type and mutant KRAS codons 12 and 13 were 8 and 13, respectively. The mutational status of KRAS remained concordant between the primary tumours and the post-FOLFOX metastatic lesions, irrespective of patient background, treatment duration and disease-free survival. Furthermore, the mutational statuses of the other genes evaluated were also concordant between the primary and metastatic lesions.

CONCLUSION: Because the mutational statuses of predictive biomarker genes were not altered by FOLFOX therapy, specimens from both primary tumours and post-FOLFOX tumour metastases might serve as valid sources of DNA for known genomic biomarker testing.

British Journal of Cancer advance online publication, 22 May 2012; doi:10.1038/bjc.2012.218 www.bjcancer.com
© 2012 Cancer Research UK

Keywords: colorectal cancer; genomic biomarker; KRAS; anti-EGFR antibody; oxaliplatin

KRAS mutations are predictive markers for the poor efficacy of anti-EGFR antibody therapies in patients with metastatic colorectal cancer (Lievre et al, 2006; Benvenuti et al, 2007; Di Fiore et al, 2007; Frattini et al, 2007; Khambata-Ford et al, 2007; Amado et al, 2008; De Roock et al, 2008; Freeman et al, 2008; Karapetis et al, 2008; Lievre et al, 2008). Point mutations in the KRAS gene occur early in the progression from colorectal adenoma to carcinoma and are detected in 35–40% of patients, regardless of their Dukes stage (Andreyev et al, 1998). More than 90% of the KRAS mutations in these patients have been detected in codons 12 (GGT) and 13 (GGC) (Oliveira et al, 2004). Activating mutations at codons 61 and 146 have also been reported in a small number of these tumours. In addition, mutations in the molecules involved in signalling pathways downstream of EGFR, such as NRAS, BRAF and PIK3CA, have also been reported in colorectal cancers. These mutations have been suggested to modify the efficacy of anti-EGFR

antibody therapies, although their predictive value has not yet been established (De Roock et al, 2010).

Oxaliplatin [trans-R,R-1,2-diaminocyclohexaneoxalatoplatinum (II), L-OHP] is a third-generation platinum (Pt)-containing anti-tumour compound. It is frequently administered as a component of FOLFOX therapy in combination with 5-FU for patients with metastatic colorectal cancer. Oxaliplatin induces DNA damage associated with intra- and inter-strand cross-links (Pt-GG adducts) and can induce gene mutations (Woynarowski et al, 2000; Hah et al, 2007; Sharma et al, 2007). The mutagenic activity of oxaliplatin has been demonstrated in cultured cells (Silva et al, 2005).

The KRAS mutation status of primary and metastatic lesions is reportedly highly concordant (Oudejans et al, 1991; Losi et al, 1992; Suchy et al, 1992; Zauber et al, 2003; Weber et al, 2007; Etienne-Grimaldi et al, 2008; Santini et al, 2008; Garm Spindler et al, 2009; Loupakis et al, 2009; Perrone et al, 2009; Baldus et al, 2010; Italiano et al, 2010; Knijn et al, 2011). However, whether long-term treatment with genotoxic chemotherapies, such as oxaliplatin, can induce additional mutations in metachronous metastatic lesions has not yet been well examined.

Assuming that FOLFOX therapy has the potential to alter the biomarker mutation profile, it is important to determine whether

the primary or relapsed tumour represents the more appropriate source of DNA for testing. We examined the mutation status of *KRAS* and other biomarker genes in primary and synchronous/ metachronous metastatic lesions in patients with stage III/IV colorectal cancer treated with adjuvant FOLFOX therapy following curative resection.

PATIENTS AND METHODS

Patient selection

A total of 63 lesions from 21 patients who had received adjuvant FOLFOX therapy for stage III/IV colorectal cancer following curative resection at the National Cancer Center Hospital East, Japan, between January 2006 and December 2009 were examined.

All patients were treated with a modified FOLFOX6 regimen, with a reduced oxaliplatin dose of $85 \, mg \, m^{-2}$ administered every 14 days, and 12 cycles were planned as the full therapy course (Andre *et al*, 2004; Allegra *et al*, 2009). FOLFOX therapy was discontinued when tumour relapse was demonstrated by imaging or when intolerable adverse events occurred.

DNA samples and mutational analyses

The DNA samples were obtained from macroscopically dissected formalin-fixed paraffin-embedded specimens cut into 10-μm-thick sections. Genomic DNA was extracted using the EZ1 Advanced XL and EZ1 DNA Tissue Kits (Qiagen, Hilden, Germany) according to the manufacturer's instructions (Bando *et al*, 2011). Mutations in *KRAS* codons 12 and 13 were detected using the ARMS/ Scorpions technology-based *KRAS* PCR Kit (Qiagen) according to the manufacturer's instructions. Mutations in *KRAS* codons 61 and 146, *NRAS* codons 12, 13 and 61, *BRAF* codon 600 and *PIK3CA* codons 542, 545, 546 and 1047 were detected using the multiplex PCR-Luminex method-based MEBGEN Mutation Kit (Medical & Biological Laboratories, Nagoya, Japan). Mutations detected with the MEBGEN Mutation Kit were confirmed by direct sequencing. Mutations in *PIK3CA* codons 542, 545 and 546 were further confirmed using the ARMS/Scorpions technology-based PI3K Mutation Test Kit (Qiagen). The study was approved by the Institutional Review Board of the National Cancer Center.

RESULTS

Patient and tumour site characteristics

We reviewed 151 consecutive cases of stage III/IV colorectal cancer treated with an adjuvant FOLFOX therapy after curative resection. Among these cases, 21 patients developed metastatic tumours that were diagnosed during or after the FOLFOX therapy and surgically resected. The patient and tumour site characteristics are shown in Table 1. The primary tumour sites were the colon and rectum in 8 and 13 patients, respectively. The most abundant primary tumour histopathological type was differentiated adenocarcinoma. Well- and moderately differentiated adenocarcinomas and mucinous adenocarcinomas were observed in 5, 14 and 2 patients, respectively. All metastatic tumours exhibited histology concordant with that of the associated primary colorectal adenocarcinoma.

In all, 12 patients had stage III disease, whereas the remaining 9 patients had synchronous metastatic lesions and were diagnosed as stage IV at the initial operation. There were 12 synchronous metastatic lesions in the patients with stage IV disease. In addition, six metastatic lesions were detected in five patients with stage III disease at operation that were resected prior to the start of FOLFOX therapy. These 18 lesions were regarded as 'pre-FOLFOX' metastatic lesions. The pre-FOLFOX metastases were found in the

Table 1 Characteristics

Patient characteristics	Number
Sex (female/male)	8/13
Median age (range)	64 (36–75) years
Primary tumour site	
Colon	8
Rectum	13
Histopathological type of primary site	
Well-differentiated adenocarcinoma	5
Moderately differentiated adenocarcinoma	14
Mucinous adenocarcinoma	2
Stage before initial operation	
III	12
IV (synchronous metastases)	9
Tumour site characteristics	
Metastases	
Pre-FOLFOX	18
Synchronous	12
Metachronous	6
Post-FOLFOX	24
Sites of metastases	
Pre-FOLFOX	
Liver	11
Lung	5
Local recurrence	1
Subcutaneous	1
Post-FOLFOX	
Liver	6
Lung	14
Local recurrence	3
Lymph node	1

liver (11 lesions), lung (5 lesions), as a local recurrence (1 lesion) and as a subcutaneous recurrence (1 lesion). Meanwhile, 24 metastatic lesions in the 21 patients were detected during or after FOLFOX therapy. These lesions were regarded as 'post-FOLFOX' metastatic lesions. The post-FOLFOX metastases were found in the liver, lung, as a local recurrence and lymph node in 6, 14, 3 and 1 patients, respectively.

The median number of FOLFOX therapy cycles administered was 9 (3–12 cycles). Five patients experienced relapse during FOLFOX therapy (case 1, 2, 3, 7 and 12), whereas the remaining 16 patients experienced relapse after the end of FOLFOX therapy. The median disease-free survival, calculated from the time of the last operation until post-FOLFOX recurrence, was 409 days (97–1077). The median period from the start of FOLFOX therapy until recurrence was 373 days (35–1029). Relapses developed within 180 days after the end of FOLFOX therapy in 10 of the 21 patients (Table 2).

Mutational status of *KRAS* and other genes

The mutational statuses of *KRAS* and other genes in primary and metastatic lesions are shown in Table 3. Mutations in *KRAS* codons 12 and 13 were detected in 13 of the 21 primary colorectal tumours. Among the remaining eight tumours with wild-type *KRAS* codons 12 and 13, two tumours exhibited *KRAS* codon 146 mutations (A146V and A146T) and one tumour exhibited *NRAS* codon 61 mutation (Q61H). Two tumours exhibited mutations in *PIK3CA* codon 542 (E542K), one tumour exhibited a *KRAS* G12S mutation and one tumour had no mutations in any of the genes examined. No apparent mutations of *KRAS* codon 61, *NRAS* codon

Table 2 FOLFOX treatment, metastasis status and tumour recurrence sites

Case	Primary site	Histopathological type	Pre-FOLFOX metastatic site	Synchronous/ metachronous	FOLFOX cycles	DFS (days)	Days from end of FOFLOX until recurrence	Post-FOLFOX recurrence site
1	Rectum	Mode	—	—	3	124	6	Liver
2	Colon	Mode	Liver	Synchronous	4	97	−16[a]	Liver
3	Colon	Mode	Liver	Synchronous	4	116	26	Liver
4	Rectum	Well	Local recurrence	Metachronous	4	469	363	Local recurrence
5	Rectum	Mode	—	—	5	827	603	Lung
6	Colon	Mode	—	—	5	350	244	Lymph node
7	Rectum	Mode	Liver	Synchronous	8	214	1	Lung
			Lung	Synchronous				
8	Rectum	Muc	—	—	8	538	318	Lung
9	Colon	Well	—	—	8	1077	903	Liver
10	Colon	Mode	Liver	Synchronous	8	344	120	Lung
			Liver	Synchronous				Lung
			Lung	Synchronous				
11	Colon	Muc	Lung	Synchronous	9	721	401	Lung
12	Rectum	Well	Liver	Synchronous	9	109	−88[a]	Liver
13	Rectum	Mode	Liver	Metachronous	11	328	120	Liver
			Lung	Metachronous				
14	Rectum	Mode	Subcutaneous	Metachronous	12	519	156	Lung
15	Colon	Mode	—		12	388	176	Local recurrence
16	Rectum	Mode	Liver	Synchronous	12	466	210	Lung
17	Rectum	Well	Lung	Synchronous	12	556	264	Lung
18	Colon·	Mode	Liver	Metachronous	12	531	231	Lung
								Lung
19	Rectum	Mode	Liver	Synchronous	12	409	217	Lung
20	Rectum	Mode	—	—	12	455	243	Local recurrence
21	Rectum	Well	Liver	Metachronous	12	346	71	Lung
								Lung

Abbreviations: DFS = disease-free survival; mode = moderately differentiated adenocarcinoma; muc = mucinous adenocarcinoma; well = well-differentiated adenocarcinoma. [a]The cases that FOLFOX therapies were administered after recurrence.

Table 3 Mutational status of KRAS and other genes

Case	Primary site	Mutation status	Pre-FOLFOX metastatic site	Mutation status	Post-FOLFOX recurrence site	Mutation status
1	Rectum	KRAS G12D	—	—	Liver	KRAS G12D
2	Colon	KRAS G12D	Liver	KRAS G12D	Liver	KRAS G12D
3	Colon	KRAS G12D	Liver	KRAS G12D	Liver	KRAS G12D
4	Rectum	KRAS G12R	Local recurrence	KRAS G12R	Local recurrence	KRAS G12R
5	Rectum	KRAS G12D	—		Lung	KRAS G12D
6	Colon	WT	—		LN	WT
7	Rectum	KRAS G12S	Liver	KRAS G12S	Lung	KRAS G12S
			Lung	KRAS G12S		
8	Rectum	WT	—	—	Lung	WT
9	Colon	WT	—		Liver	WT
10	Colon	KRAS G12A	Liver	KRAS G12A	Lung	KRAS G12A
			Liver	KRAS G12A	Lung	KRAS G12A
			Lung	WT		
11	Colon	KRAS G13D	Lung	KRAS G13D	Lung	KRAS G13D
12	Rectum	KRAS A146V	Liver	KRAS A146V	Liver	KRAS A146V
13	Rectum	KRAS G12V	Liver	KRAS G12V	Liver	KRAS G12V
			Lung	KRAS G12V		
14	Rectum	KRAS G12D	Subcutaneous	KRAS G12D	Lung	KRAS G12D
15	Colon	WT	—	—	Local recurrence	WT
16	Rectum	KRAS G12S, PIK3CA E542K	Liver	KRAS G12S, PIK3CA E542K	Lung	KRAS G12S, PIK3CA E542K
17	Rectum	KRAS G12D	Lung	KRAS G12D	Lung	KRAS G12D
18	Colon	KRAS G12D	Liver	KRAS G12D	Lung	KRAS G12D
					Lung	KRAS G12D
19	Rectum	NRAS Q61H	Liver	NRAS Q61H	Lung	NRAS Q61H
20	Rectum	PIK3CA E542K	—		Local recurrence	PIK3CA E542K
21	Rectum	KRAS A146V	Liver	KRAS A146V	Lung	KRAS A146V
					Lung	KRAS A146V

Abbreviations: LN = lymph node; WT = wild-type.